Synthesis of Cobaltaborane Clusters from $[Cp^*CoCl]_2$ and Monoboranes. New Structures and Mechanistic Implications

Yasushi Nishihara, Kathryn J. Deck, Maoyu Shang, and Thomas P. Fehlner*

Department of Chemistry and Biochemistry, University of Notre Dame, Notre Dame, Indiana 46556

Brian S. Haggerty and Arnold L. Rheingold*

Department of Chemistry and Biochemistry, University of Delaware, Newark, Delaware 19716

Received June 20, 1994®

The reaction of $[Cp^*CoCl]_2$, $Cp^* = \eta^5$-C_5Me_5, with BH_3·THF leads to the formation of *nido*-1-(η^5-C_5Me_5)Co-2-(η^4-C_5Me_5H)CoB_3H_8, **1** (60%, monoclinic $P2_1/n$, a = 8.076(1), b = 20.359(2), c = 13.880(2) Å, β = 91.23(1)°, V = 2281.7(6) Å^3, d(calcd) = 1.251g/cm^3, Z = 4), and *arachno*-(η^5-C_5Me_5)CoB_4H_{10}, **2** (2–10%, monoclinic $P2_1/c$, a = 13.954(3), b = 14.185(4), c = 29.383(7) Å, β = 100.61(2)°, V = 5717(2) Å^3, d(calcd) = 1.150 g/cm^3, Z = 16) via the metastable paramagnetic intermediate $[\{(\eta^5\text{-}C_5Me_5)Co\}(BH_3Cl)]_2$, **9**, with the coproduct BH_2Cl. Heating **1** leads to *nido*-2,4-$\{(\eta^5\text{-}C_5Me_5)Co\}_2B_3H_7$, **3** (80%, tetragonal $P4_2/n$, $a = b$ = 23.440(4), c = 8.317(2) Å, V = 4570(1) Å^3, d(calcd) = 1.244 g cm^{-3}, Z = 8). The reaction of $[Cp^*CoCl]_2$ with $LiBH_4$ leads to the formation of *closo*-2,3,4-$\{(\eta^5\text{-}C_5Me_5)Co\}_3B_2H_4$, **4** (20%, rhombohedral, $R\bar{3}$, a = 17.994 (1) Å, c = 15.986 (1) Å, V = 4477.3 Å^3, d(calcd) = 1.347 g cm^{-3}, Z = 6) and lesser amounts of *closo*-1,2,3-$\{(\eta^5\text{-}C_5Me_5)Co\}_3B_3H_5$, **5** (triclinic, $P\bar{1}$, a = 8.461 (2) Å, b = 10.718 (2) Å, c = 17.591 (4) Å, V = 1511.0 (8) Å^3, d(calcd) = 1.363 g cm^{-3}, Z = 2), and *closo*-1,2,3,6-$\{(\eta^5\text{-}C_5Me_5)Co\}_4B_2H_4$, **6**, via the sequential formation of the metastable intermediates $[\{(\eta^5\text{-}C_5Me_5)Co\}(BH_4)]_n$, **7** (paramagnetic), and $\{(\eta^5\text{-}C_5Me_5)Co\}_2B_2H_6$, **8** (diamagnetic). These results demonstrate that a labile metal precursor permits control of the number of metal atoms in the metallaborane and the characterization of unusual and metastable cobaltaboranes. A kinetic study of the conversion of **1** to **3**, which involves the intramolecular dehydrogenation of a η^4-C_5Me_5H ligand and skeletal rearrangement, is reported and the mechanistic implications for the origin of **1** are discussed.

Introduction

Most, but not all, of the known metallaboranes containing two or more metal atoms have been isolated from reaction mixtures in low yields.[1–4] Consequently, in these systems little mechanistic information connecting known reactants and any given product is available. In our own work, we have associated part of the synthetic problem with the large magnitude of the barrier for activating the reactants relative to the size of the barriers separating products.[5] Thus, the reaction of B_5H_9 with $Fe(CO)_5$ at ≈200 °C leads to low yields of monometal products.[6,7] Under milder conditions, reaction of $[H]^-$ with $Fe(CO)_5$ and BH_3·THF at room temperature leads to a complex mixture of both ferraboranes and hydrocarbyl iron clusters all of which are formed in low yields.[8] If the barrier to activating the reactants is lowered still further, greater selectivity and better yields result, i.e., the reaction of $Fe(CO)_3(cco)_2$, cco = *cis*-cyclooctene, at low temperature results in good yields of a mixture of three ferraboranes, $B_2H_6Fe_2(CO)_6$, $HFe_3(CO)_9BH_4$, and $HFe_4(CO)_{12}BH_2$, with abundances that depend directly on the Fe/B ratio.[5] Heating $B_2H_6Fe_2(CO)_6$ with BH_3·THF leads to $B_3H_7Fe_2(CO)_6$ showing that some products do have high kinetic barriers under these reaction conditions.[9] In broad mechanistic terms, the number of products are determined by the number of local minima on the potential energy surface that are accessed under the reaction conditions.[10]

This gradual progress caused us to seek even more selective routes. Thus, to form M_2B_x skeletons we sought easily activated metal dimers for reaction with monoboranes. The work of Messerle et al. suggested the reaction of $[Cp^*MCl]_2$ dimers, $Cp^* = \eta^5$-C_5Me_5, with $M'BH_4$.[11] Hence, we have explored the reaction for M = Co. M′ = Li.[12,13] As will be shown, the reaction of the dimer with BH_3·THF was equally effective since the

® Abstract published in *Advance ACS Abstracts,* October 1, 1994.

(1) Grimes, R. N. In *Metal Interactions with Boron Clusters*; Grimes, R. N., Ed.; Plenum: New York, 1982; p 269.
(2) Kennedy, J. D. *Prog. Inorg. Chem.* **1984,** *32,* 519.
(3) Kennedy, J. D. *Prog. Inorg. Chem.* **1986,** *34,* 211.
(4) Housecroft, C. E. In *Inorganometallic Chemistry*; Fehlner, T. P., Ed.; Plenum Press: New York, 1992; p 73.
(5) Meng, X.; Bandyopadhyay, A. K.; Fehlner, T. P.; Grevels, F.-W. *J. Organomet. Chem.* **1990,** *394,* 15.
(6) Greenwood, N. N.; Savory, C. G.; Grimes, R. N.; Sneddon, L. G.; Davison, A.; Wreford, S. S. *J. Chem. Soc. Chem. Commun.* **1974,** 718.
(7) Shore, S. G.; Raganini, D.; Smith, R. L.; Cottrell, C. E.; Fehlner, T. P. *Inorg. Chem.* **1979,** *18,* 670.
(8) Vites, J. C.; Housecroft, C. E.; Eigenbrot, C.; Buhl, M. L.; Long, G. J.; Fehlner, T. P. *J. Am. Chem. Soc.* **1986,** *108,* 3304.
(9) Jun, C.-S. Ph.D Thesis, University of Notre Dame, 1994.
(10) Fehlner, T. P. In *Electron Deficient Boron and Carbon Clusters*; Olah, G. A., Wade, K., Williams, R. E. Eds.; Wiley: New York, 1991; p 287.
(11) Ting, C.; Messerle, L. *J. Am. Chem. Soc.* **1989,** *111,* 3449.
(12) Deck, K. J.; Fehlner, T. P.; Rheingold, A. L. *Inorg. Chem.* **1993,** *32,* 2794.
(13) Nishihara, Y.; Deck, K. J.; Shang, M.; Fehlner, T. P. *J. Am. Chem. Soc.* **1993,** *115,* 12224.

0276-7333/94/2313-4510$04.50/0

hydride of the borane apparently readily exchanges for the chloride of the metal dimer. In both cases the byproducts present much less of a problem than did $BH_3{\cdot}PR_3$ which was generated in the formation of cobaltaboranes from $CpCo(PR_3)_2$.[14]

The synthesis and characterization of cobaltaboranes containing both CpCo, Cp = η^5-C_5H_5, and Cp*Co fragments can hardly be considered a new area and the number and types of known cobaltaboranes is large.[1-4] The lion's share of this chemistry comes from the laboratory of R. N. Grimes.[15-17] The cluster stoichiometries and structures of these compounds support the application of cluster electron counting rules[18,19] as well as isolobal ideas[20] but, importantly, also challenge them in significant instances.[21,22] There have been notable contributions from other laboratories to metallaborane and metallacarborane chemistry based on the CpCo fragment as well.[23] As expected, a number of previously characterized cobaltaboranes are observed in the present work; however, they are formed as secondary or tertiary stable products. Our choice of reaction permits the isolation of new compounds that can be cleanly converted into more stable clusters. Because of the relatively direct connection between reactants and products, significant aspects of the reaction mechanism in our system are also revealed.

Experimental Section

General Considerations. All manipulations were carried out under a nitrogen atmosphere using standard Schlenk line or dry-box techniques. Solvents were predried over 4-Å molecular sieves (tetrahydrofuran, CH_2Cl_2) or KOH (hexanes, toluene) and purged with N_2 prior to distillation. Diethyl ether, tetrahydrofuran (THF), hexanes, toluene, and pentane were distilled from sodium benzophenone ketyl. Dichloromethane was distilled from CaH_2. Hydrogen (H_2) was used directly from the tank. Baker silica gel was activated by heating at 110 °C for a several hours before chromatography was carried out. Column chromatography was performed under N_2 at −18 °C. The starting material $[Cp^*CoCl]_2$, Cp* = η^5-(C_5Me_5),[24] was prepared according to published procedures, with the modification that the anhydrous, solid $CoCl_2$ was added to a stirred THF suspension of freshly prepared $[C_5Me_5]Li$ (C_5Me_5H, Lancaster; n-BuLi, Aldrich). The air sensitive dimer was always used completely within one day of preparation, as long term storage led to decomposition. The $LiBH_4$ solution (Aldrich) was used as received and periodically titrated.[25] The metal halide was dried by heating to 130−150 °C under vacuum for at least two hours.

NMR spectra were obtained on a 300-MHz Nicolet NT-300 or GE GN-300 FT-NMR spectrometer. Residual protons of solvent were used as the reference for ^1H NMR (δ, ppm: benzene, 7.15; dichloromethane, 5.32; toluene, 2.09). For ^{13}C NMR, solvent signals were used as the chemical shift reference, while a sealed tube containing $[(NEt_4)(B_3H_8)]$ (δ −29.7 ppm) was used as the external reference for ^{11}B NMR. Infrared spectra were obtained on a Nicolet 205 FT-IR spectrometer. Mass spectra were obtained on Finnigan MAT Model 8400 or JEOL JMS-AX505HA mass spectrometers with EI, CI, and FAB (Xe, 50% *p*-nitrobenzyl alcohol and 50% glycerol) ionization modes. Perfluorokerosene was used as the standard for the high resolution EI mass spectra. Elemental analyses were carried out at Galbraith Laboratories, Knoxville, TN and M-H-W Laboratories, Phoenix, AZ.

Stable Cobaltaboranes. Syntheses: *nido*-1-(η^5-C_5Me_5)-Co-2-(η^4-C_5Me_5H)CoB_3H_8 (1) and *arachno*-(η^5-C_5Me_5)-CoB_4H_{10} (2). To a dark brown solution of 0.84 g (1.83 mmol) of $[Cp^*CoCl]_2$ in 20 mL of THF in a 200 mL round Schlenk fitted with a rubber septum[24] was added 5 equiv of $BH_3{\cdot}THF$ (1.0 M THF solution) with a 10 mL disposable syringe at −30 °C. After 8 h, the initial dark brown solution turned dark reddish-brown with a small amount of black precipitate. The solvent was evaporated in vacuo to give a dark reddish-brown oily residue. For complete removal of the solvent, 10 mL of hexane was added once. After removal of the hexane, the residue was extracted with four 20 mL portions of hexane. The hexane extract was transferred through a filter with about 1 g of Celite into another 200 mL Schlenk. After filtration, the hexane solution was concentrated to ca. 10 mL.

As chilled MeOH was circulated through its jacket at −18 °C, a 3.5 cm column was degassed and purged with N_2. Silica gel (5 cm) and hexanes were added and mixed to remove all cracks in the silica gel. A hexane solution containing product mixture was cooled in a bath of EtOH and dry ice at −20 °C to avoid the formation of precipitate in the column and then transferred to the column. The first red fraction containing mainly *nido*-1-(η^5-C_5Me_5)Co-2-(η^5-C_5Me_5H)CoB_3H_8 (1) was followed by a pale yellow fraction containing mainly *arachno*-(η^5-C_5Me_5)CoB_4H_{10} (2).

Complete separation of these two compounds is only possible by sublimation and usually the entire hexane eluate is collected and the solvent removed under vacuum. Care must be used to avoid the loss of 2 which is volatile at room temperature. 2 sublimes as pale yellow microcrystals at 29 °C (20 mg, 2% yield based on cobalt). The yield of 2 increases to 10% if the reaction solvent is changed from THF to diethyl ether. The red powder remaining after sublimation for 6 h is pure 1 (0.50 g, 60% yield based on cobalt). 1 crystallizes from hexane at low temperature as dark red plates.

Spectroscopic and analytical data for 1: HRMS (+FAB) P^+ = 430, 3 boron atoms, calcd for $^{12}C_{20}{}^1H_{39}{}^{11}B_3{}^{59}Co_2$, 430.1995, obsd, 430.2006. NMR: ^{11}B, hexanes, 22 °C, δ 6.4 (m, FWHM = 270 Hz, {^1H}, s, FWHM = 96 Hz, 1B), −4.6 (m, FWHM = 270 Hz, {^1H}, s, FWHM = 120 Hz, 2B); ^1H, CD_2Cl_2, −15 °C, δ 3.3 (partially collapsed q, BH_t), 2.50 (q, J_{HH} = 6.1 Hz, 1H), 2.26 (s, 6H), 1.92 (s, 15H, Cp*), 0.63 (s, 6H), 0.29 (d, J_{HH} = 6.2 Hz), −5.6 (br s, FWHM = 59 Hz, CoHCo), -6.0 (br s, FWHM = 130 Hz, BHB), −15.7 (partially collapsed q, CoHB); ^{13}C, C_6D_6, 18 °C, δ 98.8 (s, $(MeC)_2(CMe)_2C(H)Me$), 95.0 (s, Cp*) 60.7 (s, $(MeC)_2(CMe)_2C(H)Me$), 58.0 (d, J_{CH} = 143 Hz,$(MeC)_2$-$(CMe)_2C(H)Me$), 21.0 (q, J_{CH} = 125 Hz, $(MeC)_2(CMe)_2C(H)\mathit{Me}$), 14.0 (q, J_{CH} = 126 Hz, $(\mathit{Me}C)_2(CMe)_2C(H)Me$), 13.5 (q, J_{CH} = 127 Hz, $(MeC)_2(C\mathit{Me})_2C(H)Me$), 11.2 (q, J_{CH} = 126 Hz, Cp*). IR (pentane, cm^{-1}): 2519w, 2454 w. Anal. Calcd for $C_{20}H_{39}B_3Co_2$: C, 55.89; H, 9.15. Found: C, 56.00; H, 8.92.

Spectroscopic and analytical data for 2: HRMS (+FAB) P^+ = 248, 4 boron atoms, calcd for $^{12}C_{10}{}^1H_{25}{}^{11}B_4{}^{59}Co$, 248.1660, obsd, 248.1630. NMR: ^{11}B, hexanes, 22 °C, δ 5.1 (d, J_{BH} = 140 Hz, {^1H}, s, FWHM = 50 Hz, 2B), −5.7 (t, J_{BH} = 120 Hz, {^1H}, s, FWHM = 60 Hz, 2B); ^1H, C_6D_6, 18 °C, δ 2.8 (q, J_{BH} = 135 Hz, BH_t), 1.43 (s, 15H, Cp*), −3.9 (s, FWHM = 155 Hz, 3 BHB), −13.6 (s, FWHM = 94 Hz, 1 CoHB); ^{13}C, C_6D_6, 18 °C, δ 97.1 s, 9.2 q. IR (pentane, cm^{-1}): 2527w, 2492sh, 2443w, 2408sh.

(14) Feilong, J.; Fehlner, T. P.; Rheingold, A. L. *J. Am. Chem. Soc.* **1987**, *109*, 1860.
(15) Grimes, R. N. *Acc. Chem. Res.* **1978**, *11*, 420.
(16) Grimes, R. N. *Pure Appl. Chem.* **1982**, *54*, 43.
(17) Grimes, R. N. *Adv. Inorg. Chem. Radiochem.* **1983**, *26*, 55.
(18) Wade, K. *Adv. Inorg. Chem. Radiochem.* **1976**, *18*, 1.
(19) Mingos, D. M. P.; Johnston, R. L. *Struct. Bonding* **1987**, *68*, 29.
(20) Mingos, D. M. P.; Wales, D. J. *Introduction to Cluster Chemistry*; Prentice Hall: New York, 1990.
(21) Pipal, J. R.; Grimes, R. N. *Inorg. Chem.* **1979**, *18*, 257.
(22) Cox, D. N.; Mingos, D. M. P.; Hoffmann, R. *J. Chem. Soc., Dalton Trans.* **1981**, 1788.
(23) Micciche, R. P.; Carroll, P. J.; Sneddon, L. G. *Organometallics* **1985**, *4*, 1619.
(24) Kölle, U.; Khouzami, F.; Fuss, B. *Angew. Chem. Int. Ed. Engl.* **1982**, *21*, 131.
(25) Brown, H. C. *Organic Synthesis via Boranes*; Wiley: New York, 1975, p 241.

***nido*-2,4-{(η^5-C_5Me_5)Co}$_2B_3H_7$ (3).** The solution of 0.24 g (0.55 mmol) of **1** in 20 mL of toluene was heated at 80 °C. The bright red solution turned dark reddish black with the formation of a gas. After 2 h, the solvent was evaporated in vacuo to give a black oily residue. After hexane extraction, filtration, and concentration, column chromatography was performed as for **1** and **2**. Elution with 3% ether in hexanes gave a dark reddish black solution of *nido*-2,4-{(η^5-C_5Me_5)Co}$_2B_3H_7$ (**3**) in 80% (0.19 g) yield. In the pyrolysis, the important condition is temperature as long times or high temperatures results in lower yields.

Spectroscopic and analytical data for **3**: HRMS (EI) P^+ = 428, 3 boron atoms, calcd for $^{12}C_{20}{}^1H_{37}{}^{11}B_3{}^{59}Co_2$, 428.1838, obsd, 428.1856. NMR: ^{11}B, hexanes, 22 °C, δ 65.8 (d, J_{BH} = 116 Hz, {^{1}H}, s, FWHM = 156 Hz, 1B), −18.1 (m, FWHM = 270 Hz, {^{1}H}, s, FWHM = 120 Hz, 2B); ^{1}H, C_6D_6, 18 °C, δ 6.28 (partially collapsed q, FWHM = 390 Hz, BH_t), 1.70 (s, 15H, Cp*), −12.7 (br, FWHM = 150 Hz, BHCo); ^{13}C, C_6D_6, 18 °C, δ 89.6 s, 10.3 q. IR (pentane, cm^{-1}): 2464w, 2410w. Anal. Calcd for $C_{20}H_{37}B_3Co_2$: C, 56.16; H, 8.72. Found: C, 55.96; H, 8.75.

***closo*-2,3,4-{(η^5-C_5Me_5)Co}$_3B_2H_4$ (4).** A THF solution (10 mL) of [Cp*CoCl]$_2$ (440 mg, 0.958 mmol) was chilled to −78 °C in a dry ice−acetone bath. To the chilled brown solution was added $LiBH_4$ (1.0 mL of a 2.0 M solution; 2.0 mmol). After warming to room temperature and stirring for 24 h, the solvent was removed in vacuum. Hexane extraction yielded 258 mg of crude product after filtration and pumping. Residues after extraction are active but can be inactivated by forming a toluene slurry and slowly adding it to acetone. Column chromatography (silica gel, 4 cm ht x 3.5 cm i.d., -19 °C) of the hexane extract afforded an initial reddish band containing a mixture of **1** and **4** in hexane. Subsequent red brown hexane fractions contained only **4** (74 mg, 19% yield based on cobalt). Elution with toluene then afforded a mixture including small amounts of **3** and Cp*$_3Co_3B_4H_4$.[26] Concentration and cooling of the combined fractions containing only **4** gave a crop of crystals pure according to ^{11}B NMR (51 mg, 13%). Increasing reaction temperature increases all rates but small amounts of **6** (see below) also form. As this product is inseparable from **4**, the lower temperature reaction is required. The minor products observed at the stated reaction temperature are **1**, and Cp*$_3Co_3B_4H_4$, which are separable from **4**.

Spectroscopic and analytical data for **4**: HRMS (EI): P^+ = 608, 2 boron atoms, calcd for $^{12}C_{30}{}^1H_{49}{}^{11}B_2{}^{59}Co_3$, 608.2016, obsd, 608.2034. NMR: ^{11}B, hexanes, 22 °C, δ 104 (d, J_{BH} = 165 Hz, FWHM = 316 Hz, {^{1}H}, s, FWHM = 183 Hz); ^{1}H, $C_6D_5CD_3$, 19 °C, δ 9.6 (partially collapsed q, FWHM = 390 Hz, BH_t), 1.79 (s, FWHM = 2 Hz, Cp*), −20.8 (s, FWHM = 26 Hz, BHCo); −60 °C, δ 9.6 (s, FWHM = 95 Hz), 1.84 (s, FWHM = 3 Hz), −20.7 (s, FWHM = 14 Hz); ^{13}C{^{1}H}, $C_6D_5CD_3$, 19 °C, δ 12.0 (*C*CH$_3$), 92.2 (C*C*H$_3$). IR (hexanes, NaCl, cm^{-1}): 2451w, 2413w, BH. Anal. Calcd for $C_{30}H_{49}B_2Co_3$: C, 59.25; H, 8.12. Found: C, 59.39; H, 8.07.

***closo*-1,2,3-{(η^5-C_5Me_5)Co}$_3B_3H_5$ (5).** A hexane solution (70 mL) of [Cp*CoCl]$_2$ (0.65 g, 1.4 mmol) was chilled to −10 °C and added to a chilled hexane suspension (10 mL) of $LiBH_4$ (5.6 mmol). After stirring at room temperature for 6 days, the ^{11}B NMR indicated that the major species in solution was {(η^5-C_5Me_5)Co}$_3B_3H_5$, **5**, with minor amounts of **4**, **6**, **8** (see below), and Cp*$_3Co_3B_4H_4$. Hexane extraction, filtration, and column chromatography at −19 °C (4 cm ht x 3.5 cm d.i., silica gel, eluting solvent: hexanes/0.3% diethyl ether) afforded **5** (84 mg, 14% yield based on Co).

Spectroscopic and analytical data for **5**: MS (CI, isobutane), P^+ = 620, 2 boron atoms. NMR: ^{11}B, C_6D_6, 18 °C, δ 68.6 (d, J_{BH} = 120 Hz, FWHM = 240 Hz, {^{1}H}, s, FWHM = 100 Hz); ^{1}H, C_6D_6, 18 °C, δ 7.08 (partially collapsed q, FWHM = 290 Hz, BH_t), 1.767 (s, Cp*), −16.944 (s, FWHM = 16 Hz, BHCo); $CDCl_3$, 18 °C, δ 6.6 (partially collapsed q, FWHM = 430−460 Hz, J_{BH} ~ 250 Hz, BH_t); 1.776 (s, Cp*), −17.098 (br, FWHM = 23 Hz, BHCo); ^{13}C{^{1}H}, C_6D_6, 18 °C, δ 92.194 (*C*CH$_3$), 11.574 (C*C*H$_3$). IR (hexanes, NaCl, cm^{-1}): 2454w, 2437w, BH.

***closo*-1,2,3,6-{(η5-C_5Me_5)Co}$_4B_2H_4$ (6).** The reaction of [Cp*CoCl]$_2$ with $LiBH_4$ was carried out as for **4**. The solvent was removed under vacuum and hexane extraction was performed. Instead of being applied to a cold silica gel column immediately, the filtered extract was left in the freezer to crystallize. The major components were **4** and **8** (see below), but during several days a small amount of another product formed, and some of it precipitated. The precipitate was spectroscopically formulated as [{η^5-(C_5Me_5)Co}$_4B_2H_4$], **6**. This is the Cp* analog of (CpCo)$_4B_2H_4$ which we reported previously.[14] Attempts to prepare larger samples of pure **6** were unsuccessful.

Spectroscopic and analytical data for **6**: MS (CI, isobutane), P^+ = 802, 2 boron atoms. NMR: ^{11}B, hexanes, 18 °C, δ 128.0 (d, J_{BH} ~150 Hz); C_6D_6, 20 °C, δ 128.0 (br, FWHM = 303 Hz, {^{1}H}, s, FWHM = 227 Hz); ^{1}H, C_6D_6, 18 °C, δ 11.8 (partially collapsed q, FWHM = 430 Hz, J_{BH} ~ 170 Hz, BH_t), 1.862 (Cp*), 1.810 (Cp*), −21.79 (s, FWHM = 14 Hz, μ_3-H).

Single Crystal X-ray Diffraction Studies: *nido*-1-(η^5-C_5Me_5)Co-2-(η^4-C_5Me_5H)CoB_3H_8 (1). After column chromatography, the red solution in hexane was saturated in vacuo. Then the concentrated solution was transferred into a 5 mm tube with a constriction and placed inside a Schlenk tube. The tube was evacuated slowly and then stored in the freezer. After several weeks single crystals of **1** suitable for diffraction were found.

The compound crystallizes in monoclinic $P2_1/n$, a = 8.076(1), b = 20.359(2), c = 13.880(2) Å, β = 91.23(1)°, V = 2281.7(6) Å^3, d(calcd) = 1.251g/cm^3, Z = 4. Diffraction data were collected with an Enraf-Nonius CAD4 diffractometer equipped with a graphite crystal monochromated Mo K_α X-radiation source. Crystallographic computations were carried out on a VAX station 3200 computer using the SDP/VAX software. Cell constants and an orientation matrix for data collection were obtained from least-square refinement, using the setting angles of 25 reflections in the range 32° < 2θ < 34°. Of 7057 reflections collected, 6593 were independent and 4186 were observed. All non-hydrogen atoms were anisotropically refined and all hydrogen atoms found and refined isotropically. $R(F) = \Sigma|F_o - F_c|/\Sigma|F_o| = 4.27\%$, $R(wF) = (\Sigma w(F_o - F_c)^2/\Sigma w(F_o)^2)^{1/2} = 5.37\%$. Coordinates and selected bond distances are given in Tables 1 and 2, respectively. Other data were deposited in conjunction with the original communication.[13]

***arachno*-(η^5-C_5Me_5)CoB_4H_{10} (2).** A chromatographically purified sample in hexane was cooled to −40 °C to yield a few X-ray quality crystals. The compound crystallizes in monoclinic $P2_1/c$, a = 13.954(3), b = 14.185(4), c = 29.383(7) Å, β = 100.61(2)°, V = 5717(2) Å^3, d(calcd) = 1.150 g/cm^3, Z = 16. Diffraction data were collected with a Siemens P4 diffractometer at 242 K using Mo Kα radiation. The unit-cell dimensions were obtained from the angular settings of 25 reflections 24° < 2θ < 28°. Of 9046 data collected, 8854 were independent and 4569 were considered observed ($F_o \geq 4\sigma F_o$). Transmission ranges as a function of azimuthal angle varied by less than 10% and corrections for absorption were ignored. The structure was solved by direct methods and located the four crystallographically independent Co atoms. In two of the four independent molecules (Co 1 and Co 2), the B_4 plane is disordered and was best resolved as a planar five-membered ring of boron atoms with assigned occupancies of 0.8. All non-hydrogen atoms were refined with anisotropic thermal parameters. Hydrogen atoms were included as idealized contributions on the Cp* methyl groups and were ignored on the B_4H_{10} groups. $R(F) = 7.46\%$, $R(wF) = 9.00\%$. Coordinates and selected bond distances are given in Tables 3 and 4, respectively.

***nido*-2,4-{(η^5-C_5Me_5)Co}$_2B_3H_7$ (3).** After column chroma-

(26) Venable, T. L.; Sinn, E.; Grimes, R. N. *Inorg. Chem.* **1982**, *21*, 904.

Table 1. Positional and Equivalent Isotropic Thermal Parameters for *nido*-1-(η^5-C_5Me_5)Co-2-(η^4-C_5Me_5H)CoB_3H_8, 1

atom	x	y	z	B_{eq} (Å^2)[a,b]
C(19)	0.0497(5)	0.6435(2)	0.8177(4)	6.7(1)
C(20)	0.2277(6)	0.6435(2)	0.6162(3)	6.3(1)
B(1)	0.1046(5)	0.4477(2)	0.6000(2)	3.64(7)
B(2)	−0.0475(5)	0.4481(2)	0.7659(3)	3.89(7)
B(3)	−0.0782(5)	0.4103(2)	0.6496(3)	4.14(7)
H(1)	0.163(5)	0.436(2)	0.534(3)	3.5(9)*
H(2)	−0.113(5)	0.433(2)	0.849(3)	5(1)*
H(3)	−0.149(3)	0.375(1)	0.645(2)	0.2(5)*
H(4)	0.261(4)	0.440(2)	0.750(2)	2.2(7)*
H(5)	−0.058(4)	0.450(2)	0.580(3)	2.1(8)*
H(6)	−0.161(4)	0.449(2)	0.691(2)	2.1(8)*
H(7)	0.106(4)	0.508(2)	0.610(2)	2.1(8)*
H(8)	−0.017(5)	0.506(2)	0.763(3)	3.2(9)*
H(61)	0.564(5)	0.381(2)	0.798(3)	3.3(9)*
H(62)	0.546(5)	0.319(2)	0.853(3)	5(1)*
H(63)	0.451(6)	0.389(2)	0.895(3)	6(1)*
H(71)	0.408(5)	0.336(2)	0.551(3)	5(1)*
H(72)	0.526(5)	0.287(2)	0.599(3)	5(1)*
H(73)	0.521(5)	0.363(2)	0.631(3)	5(1)*
H(81)	0.134(5)	0.295(2)	0.511(3)	6(1)*
Co(1)	0.13395(4)	0.38819(2)	0.71688(3)	2.543(6)
Co(2)	0.16512(5)	0.51147(2)	0.72547(3)	2.753(7)
C(1)	0.3263(4)	0.3344(1)	0.7813(2)	3.29(6)
C(2)	0.3138(4)	0.3193(2)	0.6810(2)	3.23(5)
C(3)	0.1537(4)	0.2944(1)	0.6627(2)	3.36(6)
C(4)	0.0669(4)	0.2934(1)	0.7526(2)	3.39(6)
C(5)	0.1757(4)	0.3182(2)	0.8253(2)	3.42(6)
C(6)	0.4817(5)	0.3565(2)	0.8341(3)	5.12(8)
C(7)	0.4497(5)	0.3268(2)	0.6097(3)	5.23(8)
C(8)	0.0923(5)	0.2682(2)	0.5678(3)	5.29(9)
C(9)	−0.1018(4)	0.2661(2)	0.7709(3)	5.46(9)
C(10)	0.1414(6)	0.3244(2)	0.9305(3)	5.58(9)
C(11)	0.3942(4)	0.5507(2)	0.7060(2)	3.52(6)
C(12)	0.4398(4)	0.5408(2)	0.8104(2)	3.79(6)
C(13)	0.2679(4)	0.5505(2)	0.8475(2)	3.69(6)
C(14)	0.1875(4)	0.5992(2)	0.7903(2)	3.64(6)
C(15)	0.2676(4)	0.5993(1)	0.7004(2)	3.49(6)
C(16)	0.5093(5)	0.5343(2)	0.6262(3)	6.3(1)
C(17)	0.5706(5)	0.5884(2)	0.8499(3)	5.79(9)
C(18)	0.2239(7)	0.5341(3)	0.9491(3)	7.1(1)
H(82)	−0.026(5)	0.275(2)	0.574(3)	3.7(9)*
H(83)	0.122(5)	0.226(2)	0.562(3)	4(1)*
H(91)	−0.163(4)	0.263(2)	0.715(2)	2.1(7)*
H(92)	−0.173(5)	0.296(2)	0.808(3)	5(1)*
H(93)	−0.095(5)	0.224(2)	0.802(3)	5(1)*
H(101)	0.021(5)	0.329(2)	0.927(3)	5(1)*
H(102)	0.162(6)	0.289(2)	0.964(3)	7(1)*
H(103)	0.145(6)	0.366(2)	0.949(4)	7(1)*
H(121)	0.473(5)	0.497(2)	0.822(3)	2.7(8)*
H(161)	0.437(8)	0.550(2)	0.551(4)	9(2)*
H(162)	0.537(5)	0.490(2)	0.636(3)	5(1)*
H(163)	0.596(6)	0.566(2)	0.625(3)	5(1)*
H(171)	0.617(6)	0.581(2)	0.906(3)	6(1)*
H(172)	0.685(5)	0.584(2)	0.821(3)	5(1)*
H(173)	0.564(5)	0.638(2)	0.837(3)	5(1)*
H(181)	0.107(6)	0.538(2)	0.952(3)	6(1)*
H(182)	0.271(6)	0.555(2)	0.994(3)	5(1)*
H(183)	0.236(7)	0.485(3)	0.957(4)	10(2)*
H(191)	−0.027(5)	0.627(2)	0.846(3)	4(1)*
H(192)	−0.024(5)	0.650(2)	0.761(3)	3.1(9)*
H(193)	0.082(5)	0.681(2)	0.856(3)	5(1)*
H(201)	0.246(7)	0.620(3)	0.550(4)	9(2)*
H(202)	0.116(5)	0.652(2)	0.611(3)	3.6(9)*
H(203)	0.275(6)	0.689(3)	0.631(4)	8(2)*

[a] Starred atoms were refined isotropically. [b] Anisotropically refined atoms are given in the form of the isotropic equivalent displacement parameter defined as: $^4/_3[a^2B(1,1) + b^2B(2,2) + c^2B(3,3) + ab(\cos\gamma)B(1,2) + ac(\cos\beta)B(1,3) + bc(\cos\alpha)B(2,3)]$.

tography, the hexane solution of **3** was concentrated by reduced pressure in a Schlenk tube. Then the tube was stored at 0 °C for several days, followed by cooling gradually from 0 °C to −40 °C over two weeks. The mother liquor was transferred at low temperature into another Schlenk tube. A black solid was isolated from remaining solvent by slow evaporation. After that, a single crystal of **3** was obtained as a black column.

Table 2. Selected Bond Distances (Å) and Angles (deg) for *nido*-1-(η^5-C_5Me_5)Co-2-(η^4-C_5Me_5H)CoB_3H_8, 1

Co(1)−C(1)	2.085(3)	Co(2)−H(4)	1.68(3)
Co(1)−C(2)	2.087(3)	Co(2)−H(7)	1.66(3)
Co(1)−C(3)	2.061(3)	Co(2)−H(8)	1.58(4)
Co(1)−C(4)	2.069(3)	B(1)−H(1)	1.06(4)
Co(1)−C(5)	2.095(3)	B(1)−H(5)	1.33(4)
Co(1)−B(1)	2.035(3)	B(1)−H(7)	1.23(4)
Co(1)−B(2)	2.035(4)	B(2)−H(2)	1.31(4)
Co(1)−B(3)	1.984(4)	B(2)−H(6)	1.38(3)
Co(1)−H(4)	1.53(3)	B(2)−H(8)	1.20(4)
Co(2)−C(11)	2.038(3)	B(3)−H(3)	0.92(3)
Co(2)−C(13)	2.032(3)	B(3)−H(5)	1.28(3)
Co(2)−C(14)	2.006(3)	B(3)−H(6)	1.20(3)
Co(2)−C(15)	2.005(3)		
B(1)−Co(1)−B(2)	80.7(2)	H(2)−B(2)−H(6)	113(2)
B(1)−Co(1)−B(3)	53.5(2)	H(2)−B(2)−H(8)	110(3)
B(1)−Co(1)−H(4)	84(1)	Co(1)−B(3)−H(5)	112(2)
B(2)−Co(1)−B(3)	53.2(2)	Co(1)−B(3)−H(6)	114(2)
B(2)−Co(1)−H(4)	88(1)	H(3)−B(3)−H(5)	122(2)
B(3)−Co(1)−H(4)	123(1)	H(3)−B(3)−H(6)	102(2)
H(4)−Co(2)−H(7)	106(2)	H(5)−B(3)−H(6)	91(2)
H(4)−Co(2)−H(8)	107(2)	Co(1)−H(4)−Co(2)	103(2)
H(7)−Co(2)−H(8)	94(2)	B(1)−H(5)−B(3)	88(2)
Co(1)−B(1)−H(7)	120(2)	B(2)−H(6)−B(3)	89(2)
H(1)−B(1)−H(5)	106(3)	Co(2)−H(7)−B(1)	99(2)
H(1)−B(1)−H(7)	109(3)	Co(1)−B(1)−H(1)	120(2)
H(5)−B(1)−H(7)	90(2)	Co(1)−B(1)−H(5)	107(1)
Co(1)−B(2)−H(2)	117(2)	H(6)−B(2)−H(8)	95(2)
Co(1)−B(2)−H(6)	103(1)	Co(1)−B(3)−H(3)	112(2)
Co(1)−B(2)−H(8)	115(2)	Co(2)−H(8)−B(2)	106(3)

3 crystallizes in tetragonal $P4_2/n$, $a = b = 23.440(4)$, $c = 8.317(2)$ Å, $V = 4570(1)$ Å^3, d(calcd) = 1.244 g cm^{-3}, $Z = 8$. Diffraction data were collected with an Enraf-Nonius CAD4 diffractometer equipped with a graphite crystal monochromated Mo K_α X-radiation source at 293 K. Crystallographic computations were carried out on a VAX station 3200 computer using the SDP/VAX software. Cell constants and an orientation matrix for data collection were obtained from least-square refinement, using the setting angles of 25 reflections in the range $31° < 2\theta < 32°$, measured by the computer controlled diagonal slit method of centering. Of 3360 reflections collected, 3156 were independent and 2076 were observed. All non-hydrogen atoms were anisotropically refined and all hydrogen atoms found and either refined isotropically or involved only in the structure factor calculation. $R(F) = 3.49\%$, $R(wF) = 4.23\%$. Coordinates and selected bond distances are given in Tables 5 and 6, respectively. Other data were deposited in conjunction with the original communication.[13]

***closo*-2,3,4-{(η^5-C_5Me_5)Co}$_3B_2H_4$ (4).** Suitable crystals were grown by slow cooling of a hexanes solution. **1** crystallizes in rhombohedral, $R\bar{3}$, $a = 17.994(1)$ Å, $c = 15.986$ (1) Å, $V = 4477.3$ Å^3, d(calcd) = 1.347 g cm^{-3}, $Z = 6$. Of 1965 reflections collected (Siemens P4 diffractometer, Mo Kα, 295 K), 1786 were independent and 1263 were observed ($5\sigma(F_o)$). With all non-hydrogen atoms anisotropically refined and all methyl-group hydrogen atoms idealized (the axial BH atoms were found but not the bridging ones): $R(F) = 4.28\%$, $R(wF) = 5.66\%$. Coordinates and selected bond distances are given in Tables 7 and 8, respectively. Other data were deposited in conjunction with the original communication.[12]

***closo*-1,2,3-{(η^5-C_5Me_5)Co}$_3B_3H_5$ (5).** Suitable crystals were grown by slow evaporation of a toluene-d_8 solution in a 5-mm tube at room temperature. Crystallographic data: $C_{30}H_{50}Co_3B_3$, triclinic, $P\bar{1}$, $a = 8.461$ (2) Å, $b = 10.718$ (2) Å, $c = 17.591(4)$ Å, $V = 1511.0(8)$ Å^3, d(calcd) = 1.363 g cm^{-3}, $Z = 2$. Of 4200 unique reflections collected (Enraf-Nonius CAD4 diffractometer), 3346 (with $F_o^2 > 3.0\sigma(F_o^2)$) were used in the refinements. After non-hydrogen atoms and hydrogen atoms were refined anisotropically and isotropically, respectively, to

Table 3. Atomic Coordinates ($\times 10^4$) and Equivalent Isotropic Displacement Coefficients ($Å^2 \times 10^3$) for *arachno*-(η^5-C_5Me_5)CoB_4H_{10}, 2

	x	y	z	U_{eq}[a]
Co(1)	129(1)	6059(1)	2539(1)	56(1)
C(10)	305(7)	4839(6)	2911(3)	55(2)
C(11)	926(6)	4824(6)	2594(4)	50(2)
C(12)	367(7)	4905(6)	2163(3)	57(2)
C(13)	−627(7)	4959(5)	2209(4)	59(2)
C(14)	−678(6)	4894(6)	2665(4)	63(2)
C(15)	582(9)	4716(8)	3433(3)	116(2)
C(16)	1985(7)	4691(8)	2729(4)	106(2)
C(17)	761(9)	4849(8)	1729(4)	115(2)
C(18)	−1443(7)	4962(7)	1791(4)	121(2)
C(19)	−1568(8)	4859(8)	2849(5)	138(2)
B(11)	1096(15)	7081(13)	2399(9)	136(2)
B(12)	−58(13)	7150(11)	2082(6)	93(2)
B(13)	−893(12)	7106(10)	2455(6)	83(2)
B(14)	−159(13)	7012(12)	3029(8)	115(2)
B(15)	970(16)	6991(15)	2971(10)	171(2)
Co(2)	4613(1)	2524(1)	4566(1)	52(1)
C(20)	3606(6)	2000(7)	4934(3)	51(2)
C(21)	3381(5)	1690(6)	4466(3)	50(2)
C(22)	3219(5)	2512(7)	4186(3)	46(1)
C(23)	3357(5)	3297(6)	4473(3)	50(2)
C(24)	3591(6)	2987(7)	4943(3)	49(2)
C(25)	3766(7)	1372(7)	5356(4)	89(2)
C(26)	3264(7)	680(6)	4314(4)	90(2)
C(27)	2883(7)	2507(7)	3676(3)	82(2)
C(28)	3197(7)	4309(7)	4311(4)	89(2)
C(29)	3721(7)	3623(7)	5355(3)	84(2)
B(21)	5406(12)	1965(18)	4123(7)	159(2)
B(22)	5691(13)	1541(14)	4651(11)	169(2)
B(23)	5865(12)	2300(19)	5034(10)	236(2)
B(24)	5726(12)	3341(17)	4769(10)	229(2)
B(25)	5378(13)	3284(16)	4153(8)	147(2)
Co(3)	321(1)	7459(1)	143(1)	67(1)
C(30)	1619(6)	7512(9)	598(3)	75(2)
C(31)	1542(6)	8267(6)	288(5)	69(2)
C(32)	1458(6)	7923(9)	−145(4)	81(2)
C(33)	1475(6)	6952(9)	−115(5)	90(2)
C(34)	1580(7)	6698(7)	334(5)	77(2)
C(35)	1820(9)	7437(12)	1123(4)	209(2)
C(36)	1647(9)	9242(8)	489(7)	248(2)
C(37)	1400(9)	8606(11)	−545(5)	207(2)
C(38)	1445(9)	6371(11)	−557(5)	191(2)
C(39)	1685(8)	5696(8)	462(6)	209(2)
B(31)	−615(10)	6702(13)	472(7)	150(2)
B(32)	−652(9)	8139(15)	435(8)	175(2)
B(33)	−799(10)	8140(12)	−239(8)	158(2)
B(34)	−767(10)	6869(15)	−287(10)	249(2)
Co(4)	4989(1)	2474(1)	2162(1)	61(1)
C(40)	4512(10)	3301(6)	1594(3)	83(2)
C(41)	3838(7)	2580(10)	1621(3)	90(2)
C(42)	4337(8)	1720(7)	1596(3)	77(2)
C(43)	5260(7)	1945(8)	1546(3)	67(2)
C(44)	5353(7)	2913(9)	1548(3)	74(2)
C(45)	4178(12)	4287(8)	1593(4)	232(2)
C(46)	2750(8)	2618(12)	1649(5)	215(2)
C(47)	3891(10)	753(9)	1585(4)	179(2)
C(48)	5993(9)	1240(10)	1461(4)	179(2)
C(49)	6196(9)	3484(11)	1472(4)	187(2)
B(41)	5919(12)	3223(15)	2639(6)	166(2)
B(42)	4608(11)	3179(12)	2697(5)	110(2)
B(43)	4518(11)	1853(12)	2694(5)	110(2)
B(44)	5790(12)	1598(13)	2629(6)	148(2)

[a] Equivalent isotropic U defined as one-third of the trace of the orthogonalized U_{ij} tensor.

convergence, a difference Fourier synthesis showed a peak with the electron density of about a hydrogen, which capped the three cobalt atoms. Refinement of the peak as a hydrogen atom resulted in negative thermal parameters, while assignment as a boron atom yielded an unusually high thermal parameter, 35 Å^2. The peak was assigned as a boron atom with partial occupancy, which converged to 23% along with a comparable thermal parameter to those of the other boron atoms in the ensuing refinement. This is consistent with the fact that the single crystals were grown from a solution containing 85% **5** and 15% [$(Cp^*Co)_3B_4H_4$] by ^{1}H NMR. The two bridging hydrides and methyl hydrogen atoms were not located from difference Fourier syntheses. $R(F) = 5.056\%$; $R(wF) = 7.382\%$. Coordinates and selected bond distances are given in Tables 9 and 10, respectively.

Table 4. Selected Bond Distances (Å) and Angles (deg) for *arachno*-(η^5-C_5Me_5)CoB_4H_{10}, 2

Co(4)−C(41)	2.046(9)	Co(4)−C(40)	2.048(10)
Co(4)−C(43)	2.058(10)	Co(4)−C(42)	2.044(9)
Co(4)−B(41)	2.028(17)	Co(4)−C(44)	2.059(11)
Co(4)−B(43)	2.007(16)	Co(4)−B(42)	2.015(16)
C(40)−C(41)	1.401(17)	Co(4)−B(44)	2.027(17)
C(40)−C(45)	1.474(16)	C(40)−C(44)	1.326(17)
C(41)−C(46)	1.537(16)	C(41)−C(42)	1.413(17)
C(42)−C(47)	1.504(16)	C(42)−C(43)	1.362(16)
C(43)−C(48)	1.484(17)	C(43)−C(44)	1.380(16)
B(41)−B(42)	1.870(24)	C(44)−C(49)	1.478(18)
B(43)−B(44)	1.856(23)	B(42)−B(43)	1.885(24)
Co(4)−B(42)−B(41)	62.8(8)	C(42)−Co(4)−B(44)	109.7(6)
B(41)−B(42)−B(43)	95.6(11)	C(44)−Co(4)−B(44)	125.7(6)
Co(4)−B(43)−B(44)	63.2(7)	B(41)−Co(4)−B(44)	69.5(8)
Co(4)−B(44)−B(43)	62.1(7)	B(43)−Co(4)−B(44)	54.8(7)
Co(4)−B(41)−B(42)	62.1(7)	B(42)−Co(4)−B(43)	55.9(7)
Co(4)−B(42)−B(43)	61.8(7)	B(41)−Co(4)−B(42)	55.1(7)
Co(4)−B(43)−B(42)	62.3(7)	B(41)−Co(4)−B(43)	87.2(7)
B(42)−B(43)−B(44)	97.5(11)	B(42)−Co(4)−B(44)	88.2(7)
C(40)−Co(4)−B(44)	163.4(7)		

Table 5. Positional and Equivalent Isotropic Thermal Parameters for *nido*-2,4-{(η^5-C_5Me_5)Co}$_2B_3H_7$, 3

atom	x	y	z	B_{eq} (Å^2)[a,b]
Co(1)	0.22214(2)	0.03101(2)	0.08088(7)	4.19(1)
Co(2)	0.31610(2)	−0.06825(2)	−0.03882(8)	4.21(1)
C(1)	0.2260(2)	0.0924(2)	0.2547(6)	4.6(1)
C(2)	0.2304(2)	0.1170(2)	0.1012(6)	4.9(1)
C(3)	0.1808(2)	0.1032(2)	0.0135(5)	5.3(1)
C(4)	0.1449(2)	0.0711(2)	0.1146(6)	5.1(1)
C(5)	0.1722(2)	0.0636(2)	0.2618(6)	4.7(1)
C(6)	0.2679(2)	0.0971(3)	0.3904(8)	8.5(2)
C(7)	0.2792(3)	0.1539(2)	0.0461(9)	9.1(2)
C(8)	0.1667(3)	0.1211(3)	−0.1553(7)	10.3(2)
C(9)	0.0859(2)	0.0479(3)	0.0745(8)	9.3(2)
C(10)	0.1498(3)	0.0328(3)	0.4067(7)	8.3(2)
C(11)	0.3951(2)	−0.0597(2)	−0.1278(6)	6.1(1)
C(12)	0.3980(2)	−0.0815(2)	0.0262(6)	5.3(1)
C(13)	0.3696(2)	−0.1323(2)	0.0296(6)	5.5(1)
C(14)	0.3490(2)	−0.1450(2)	−0.1175(6)	5.7(1)
C(15)	0.3630(2)	−0.1016(3)	−0.2217(6)	7.2(1)
C(16)	0.4214(3)	−0.0042(3)	−0.181(1)	15.9(2)
C(17)	0.4291(3)	−0.0556(3)	0.1689(9)	12.7(2)
C(18)	0.3630(3)	−0.1675(3)	0.1860(9)	12.8(2)
C(19)	0.3159(3)	−0.2007(3)	−0.150(1)	13.8(2)
C(20)	0.3502(4)	−0.0967(5)	−0.3976(9)	20.2(4)
B(1)	0.3032(2)	0.0096(2)	0.0464(7)	4.9(1)
B(2)	0.2672(3)	0.0018(3)	−0.1262(8)	7.9(2)
B(3)	0.2691(3)	−0.0406(3)	0.1657(8)	8.1(2)
H(1)	0.334(2)	0.035(2)	0.076(5)	4(1)*
H(2)	0.273(3)	0.029(2)	−0.246(8)	12(2)*
H(3)	0.283(3)	−0.048(3)	0.284(8)	11(2)*
H(4)	0.214(2)	−0.007(2)	−0.088(6)	5(1)*
H(5)	0.219(2)	−0.025(2)	0.126(7)	7(1)*
H(6)	0.265(2)	−0.048(2)	−0.142(7)	8(1)*
H(7)	0.266(2)	−0.088(2)	0.059(6)	6(1)*

[a] Starred atoms were refined isotropically. [b] Anisotropically refined atoms are given in the form of the isotropic equivalent displacement parameter defined as $^4/_3[a^2B(1,1) + b^2B(2,2) + c^2B(3,3) + ab(\cos\gamma)B(1,2) + ac(\cos\beta)B(1,3) + bc(\cos\alpha)B(2,3)]$.

Metastable Cobaltaboranes. [{(η^5-C_5Me_5)Co}(BH_4)]$_n$ (7). A THF solution (32 mL) of [Cp*CoCl]$_2$ (1.462 g, 3.2 mmol) was chilled below −50 °C. To it was added $LiBH_4$ (3.2 mL of 2.0 M solution: 6.4 mmol). After stirring at −40 °C for 30 min, the temperature was raised to 0 °C and held there for 45 min. Effervescence was observed at 0 °C. After 15 min more at 0−10 °C, the solvent was removed under vacuum. The flask

Table 6. Selected Bond Distances (Å) and Angles (deg) for *nido*-2,4-{(η^5-C_5Me_5)Co}$_2B_3H_7$, 3

Co(1)−C(1)	2.041(4)	Co(2)−B(1)	1.980(5)
Co(1)−C(2)	2.033(4)	Co(2)−H(6)	1.54(5)
Co(1)−C(3)	2.028(4)	Co(2)−H(7)	1.50(5)
Co(1)−C(4)	2.059(4)	B(1)−B(2)	1.674(9)
Co(1)−C(5)	2.052(5)	B(1)−B(3)	1.733(8)
Co(1)−B(1)	1.986(5)	H(1)−B(1)	0.97(4)
Co(1)−H(4)	1.67(5)	H(2)−B(2)	1.19(6)
Co(1)−H(5)	1.37(5)	H(3)−B(3)	1.05(7)
Co(2)−C(11)	2.004(5)	H(4)−B(2)	1.29(4)
Co(2)−C(12)	2.019(4)	H(5)−B(3)	1.27(5)
Co(2)−C(13)	2.038(4)	H(6)−B(2)	1.18(5)
Co(2)−C(14)	2.063(5)	H(7)−B(3)	1.42(5)
Co(2)−C(15)	2.033(5)		
B(1)−Co(1)−H(4)	81(1)	Co(2)−B(1)−B(2)	70.8(3)
B(1)−Co(1)−H(5)	81(2)	Co(2)−B(1)−B(3)	69.5(3)
B(1)−Co(2)−H(6)	78(2)	B(2)−B(1)−B(3)	100.6(4)
B(1)−Co(2)−H(7)	88(2)	B(2)−B(1)−B(3)	100.6(4)
H(4)−Co(1)−H(5)	74(3)	Co(1)−H(4)−B(2)	91(3)
H(6)−Co(2)−H(7)	78(3)	Co(1)−H(5)−B(3)	108(3)
Co(1)−B(1)−Co(2)	115.6(2)	Co(2)−H(6)−B(2)	102(4)
Co(1)−B(1)−B(2)	70.7(3)	Co(2)−H(7)−B(3)	94(3)
Co(1)−B(1)−B(3)	69.4(3)		

Table 7. Atomic Coordinates (×10^4) and Equivalent Isotropic Displacement Coefficients (Å^2 × 10^3) for *closo*-2,3,4-{(η^5-C_5Me_5)Co}$_3B_2H_4$, 4

	x	y	z	U_{eq}[a]
Co	6062(1)	2421(1)	676(1)	36(1)
C(1)	5148(3)	1439(3)	1441(3)	47(2)
C(2)	4765(3)	1468(3)	675(3)	47(2)
C(3)	5197(3)	1319(3)	13(3)	46(2)
C(4)	5847(3)	1199(3)	355(3)	40(2)
C(5)	5821(3)	1276(3)	1254(3)	44(2)
C(6)	4843(4)	1481(4)	2306(4)	79(4)
C(7)	3962(3)	1513(4)	585(5)	76(3)
C(8)	4965(4)	1239(4)	−899(4)	71(3)
C(9)	6396(4)	945(3)	−138(4)	64(3)
C(10)	6355(4)	1123(4)	1875(4)	71(3)
B(1)	6667	3333	−200(7)	54(3)
B(2)	6667	3333	1527(6)	40(3)

[a] Equivalent isotropic U defined as one-third of the trace of the orthogonalized U_{ij} tensor.

Table 8. Selected Bond Distances (Å) and Angles (deg) for *closo*-2,3,4-{(η^5-C_5Me_5)Co}$_3B_2H_4$, 4

Co−C(1)	2.101(4)	Co−C(2)	2.094(4)
Co−C(3)	2.095(4)	Co−C(4)	2.096(5)
Co−C(5)	2.095(5)	Co−B(1)	2.013(8)
Co−B(2)	1.985(6)	Co−CoA	2.507(1)
Co−CoB	2.507(1)	C(1)−C(2)	1.419(8)
C(1)−C(5)	1.413(9)	C(1)−C(6)	1.504(8)
C(2)−C(3)	1.416(8)	C(2)−C(7)	1.494(9)
C(3)−C(4)	1.402(8)	C(3)−C(8)	1.504(8)
C(4)−C(5)	1.446(7)	C(4)−C(9)	1.503(10)
C(5)−C(10)	1.500(9)	B(1)−CoA	2.013(8)
B(1)−CoB	2.014(8)	B(2)−CoA	1.985(6)
B(2)−CoB	1.986(6)		
B(1)−Co−B(2)	87.3(3)	B(2)−Co−CoA	50.8(1)
C(2)−Co−CoA	175.7(2)	C(2)−Co−CoB	115.7(2)
C(4)−Co−CoA	117.9(1)	C(4)−Co−CoB	165.8(1)
B(1)−Co−CoA	51.5(2)	B(1)−Co−CoB	51.5(2)
C(1)−Co−CoB	124.5(2)	CoA−Co−CoB	60.0(1)
C(3)−Co−CoB	133.1(2)	Co−B(1)−CoA	77.0(4)
C(5)−Co−CoB	153.8(1)	CoA−B(1)−CoB	77.0(4)
B(2)−Co−CoB	50.9(1)	Co−B(2)−CoB	78.3(3)
C(1)−Co−CoA	142.1(1)	Co−B(1)−CoB	77.0(4)
C(3)−Co−CoA	142.9(1)	Co−B(2)−CoA	78.3(3)
C(5)−Co−CoA	117.5(1)	CoA−B(2)−CoB	78.3(3)

remained cold during pumping. Hexane extraction was carried out and an aliquot was removed immediately for ^{1}H NMR. The most prominent signals in the ^{1}H NMR spectrum were at δ +66 ppm (Cp* signal of the paramagnetic intermediate, **7**) and 1.747 ppm (Cp* signal of a subsequent diamagnetic product, **8**, see below). Crystallization of concentrated hexanes solutions at −40 °C gave dark brown, microcrystalline solids.

Table 9. Positional and Equivalent Isotropic Thermal Parameters for *closo*-1,2,3-{(η^5-C_5Me_5)Co}$_3B_3H_5$, 5

atom	x	y	z	B_{eq} (Å^2)[a]
Co(1)	0.71530(8)	0.58705(6)	0.75728(4)	2.66(1)
Co(2)	0.69465(8)	0.81434(7)	0.81037(4)	2.80(2)
Co(3)	0.66640(9)	0.78158(7)	0.66817(4)	2.94(2)
B(1)	0.9012(8)	0.6591(7)	0.7815(4)	3.6(2)
B(2)	0.8847(9)	0.6369(7)	0.6864(4)	3.6(2)
B(3)	0.8732(8)	0.7892(7)	0.7213(4)	3.9(2)
C(1)	0.8408(8)	0.3921(6)	0.7688(5)	5.3(2)
C(2)	0.7331(9)	0.4053(6)	0.7096(4)	5.2(2)
C(3)	0.5694(7)	0.4603(5)	0.7422(4)	4.2(1)
C(4)	0.5765(7)	0.4804(6)	0.8195(4)	4.1(1)
C(5)	0.7390(9)	0.4390(6)	0.8367(4)	4.8(2)
C(6)	1.030(1)	0.3294(8)	0.764(1)	12.8(5)
C(7)	0.784(2)	0.3560(8)	0.6273(5)	11.7(3)
C(8)	0.408(1)	0.4753(8)	0.7047(6)	9.3(2)
C(9)	0.424(1)	0.5255(8)	0.8763(5)	8.8(2)
C(10)	0.806(1)	0.4247(9)	0.9162(5)	11.0(3)
C(11)	0.639(1)	1.0042(6)	0.8508(4)	9.0(3)
C(12)	0.5094(9)	0.9650(7)	0.8732(4)	6.0(2)
C(13)	0.562(1)	0.8666(7)	0.9174(4)	7.4(2)
C(14)	0.726(1)	0.8369(8)	0.9237(4)	9.4(2)
C(15)	0.7789(9)	0.9246(8)	0.8805(5)	10.2(2)
C(16)	0.682(3)	1.115(1)	0.8101(8)	35.8(7)
C(17)	0.339(2)	1.043(2)	0.8526(7)	23.4(5)
C(18)	0.418(2)	0.817(1)	0.9561(7)	21.2(4)
C(19)	0.795(3)	0.730(1)	0.9817(7)	24.8(8)
C(20)	0.962(1)	0.895(1)	0.8953(9)	29.3(4)
C(21)	0.719(1)	0.846(1)	0.5637(4)	8.3(2)
C(22)	0.644(1)	0.7480(8)	0.5542(4)	6.7(2)
C(23)	0.4880(9)	0.7919(7)	0.5867(4)	5.5(2)
C(24)	0.458(1)	0.9093(7)	0.6175(4)	5.9(2)
C(25)	0.600(1)	0.9485(6)	0.6032(4)	8.8(2)
C(26)	0.893(1)	0.839(2)	0.5289(7)	19.8(5)
C(27)	0.723(2)	0.622(1)	0.5044(6)	16.1(5)
C(28)	0.355(1)	0.724(1)	0.5828(7)	13.0(3)
C(29)	0.293(2)	0.993(2)	0.6566(7)	19.8(5)
C(30)	0.631(2)	1.078(1)	0.6182(8)	24.2(5)
H(1)	0.993(8)	0.616(6)	0.824(4)	4(2)[b]
H(2)	0.962(9)	0.560(7)	0.640(4)	5(2)[b]
H(3)	0.922(8)	0.855(6)	0.706(4)	3(2)[b]
B(4)	0.533(4)	0.748(3)	0.758(2)	3.7(6)[b,c]

[a] Anisotropically refined atoms are given in the form of the isotropic equivalent displacement parameter defined as $^4/_3[a^2B(1,1) + b^2B(2,2) + c^2B(3,3) + ab(\cos\gamma)B(1,2) + ac(\cos\beta)B(1,3) + bc(\cos\alpha)B(2,3)]$. [b] Atom was refined isotropically. [c] Occupancy was 0.23.

Spectroscopic data for (**7**). NMR: ^{11}B, hexanes, 22 °C, δ −176 ppm (s, FWHM = 220 Hz, {^{1}H}, s, FWHM = 180 Hz), THF, 22 °C, δ −182 ppm (s, FWHM = 250 Hz). A temperature-dependent chemical shift and broadening at low temperature was observed: ^{1}H, $C_6D_5CD_3$, −90 °C, δ 111 ppm (FWHM = 860 Hz); -60 °C, δ 94 ppm (FWHM = 430 Hz); −30 °C, δ 81 ppm (FWHM = 300 Hz); 0 °C, δ 72 ppm (FWHM = 210 Hz); 18 °C, δ 66 ppm (FWHM = 190 Hz) (br s, Cp*).

{(η^5-C_5Me_5)Co}$_2B_2H_6$ (8). Low temperature chromatography of a 30-min reaction of [Cp*CoCl]$_2$ with 2 $LiBH_4$ in THF gives pure [(Cp*Co)$_2B_2H_6$] (as a mixture of two tautomers in solution) in low yield. A large scale (1.46 g [Cp*CoCl]$_2$, 3.2 mmol; 6.4 mmol $LiBH_4$) reaction at low temperature, followed by rapid workup (hexane extraction) and quick crystallization (very concentrated solution, cooled to −40 °C overnight) gives larger amounts of [(Cp*Co)$_2B_2H_6$] of lower purity (major impurity is **7**).

Spectroscopic and analytical data for (**8**). MS (EI): P$^+$ = 416, 2 boron atoms. NMR: ^{11}B, hexanes, 18 °C, δ −7.5 (s, FWHM = 190 Hz, {^{1}H}, s, FWHM = 160 Hz), 51.0 (d, FWHM = 260 Hz, J = 110 Hz, {^{1}H}, s, FWHM = 150 Hz); ^{1}H, C_6D_6, 18 °C, δ ~3.7 (partially collapsed q, J ~ 140 Hz, BH_t), 1.747 (s, FWHM = 6 Hz, Cp*), −10.6 (br s, FWHM = 380 Hz, BHCo), −16.0 (br s, FWHM = 260 Hz, BHCo). IR (KBr, cm^{-1}): 2456w, 2409w, BH.

Table 10. Selected Bond Distances (Å) and Angles (deg) for *closo*-1,2,3-{(η^5-C_5Me_5)Co}$_3B_3H_5$, 5

Co(1)−Co(2)	2.561(1)	Co(2)−C(14)	2.054(8)
Co(1)−Co(3)	2.551(1)	Co(2)−C(15)	2.020(9)
Co(1)−B(1)	2.026(8)	Co(3)−B(2)	2.049(6)
Co(1)−B(2)	2.032(8)	Co(3)−B(3)	2.062(8)
Co(1)−C(1)	2.042(5)	Co(3)−C(21)	2.033(8)
Co(1)−C(2)	2.081(6)	Co(3)−C(22)	2.069(7)
Co(1)−C(3)	2.130(7)	Co(3)−C(23)	2.129(7)
Co(1)−C(4)	2.131(7)	Co(3)−C(24)	2.115(7)
Co(1)−C(5)	2.083(6)	Co(3)−C(25)	2.067(7)
Co(2)−Co(3)	2.564(1)	B(1)−B(2)	1.71(1)
Co(2)−B(1)	2.035(6)	B(1)−B(3)	1.71(1)
Co(2)−B(3)	2.058(7)	B(1)−H(1)	1.10(7)
Co(2)−C(11)	2.056(7)	B(2)−B(3)	1.72(1)
Co(2)−C(12)	2.115(7)	B(2)−H(2)	1.16(7)
Co(2)−C(13)	2.107(7)	B(3)−H(3)	0.95(7)
Co(2)−Co(1)−Co(3)	60.22(3)	Co(2)−B(1)−B(2)	102.6(4)
Co(2)−Co(1)−B(1)	51.0(2)	Co(2)−B(1)−B(3)	65.9(3)
Co(2)−Co(1)−B(2)	78.3(2)	Co(1)−B(2)−Co(3)	77.4(2)
Co(3)−Co(1)−B(1)	78.4(2)	Co(2)−B(3)−H(3)	123(4)
Co(3)−Co(1)−B(2)	51.6(2)	Co(3)−B(3)−B(1)	100.9(5)
B(1)−Co(1)−B(2)	49.9(3)	Co(3)−B(3)−B(2)	64.9(4)
Co(1)−Co(2)−Co(3)	59.68(3)	Co(3)−B(3)−H(3)	118(4)
Co(1)−Co(2)−B(1)	50.8(2)	B(1)−B(3)−B(2)	59.9(4)
Co(1)−Co(2)−B(3)	77.8(2)	B(1)−B(3)−H(3)	141(4)
Co(3)−B(2)−B(1)	101.5(3)	B(2)−B(3)−H(3)	135(4)
Co(3)−B(2)−B(3)	65.7(3)	Co(1)−B(2)−B(1)	64.9(3)
Co(3)−B(2)−H(2)	124(4)	Co(2)−B(1)−H(1)	121(3)
B(1)−B(2)−B(3)	60.0(4)	B(2)−B(1)−B(3)	60.1(4)
B(1)−B(2)−H(2)	134(4)	B(2)−B(1)−H(1)	136(3)
B(3)−B(2)−H(2)	139(4)	B(3)−B(1)−H(1)	134(4)
Co(2)−B(3)−Co(3)	77.0(2)	Co(1)−B(2)−B(3)	102.4(4)
Co(2)−B(3)−B(1)	64.5(3)	Co(1)−B(2)−H(2)	118(4)
Co(2)−B(3)−B(2)	101.5(4)	Co(3)−Co(2)−B(1)	77.9(2)
Co(2)−Co(3)−B(3)	51.4(2)	Co(3)−Co(2)−B(3)	51.6(2)
B(2)−Co(3)−B(3)	49.4(3)	B(1)−Co(2)−B(3)	49.5(3)
Co(1)−B(1)−Co(2)	78.2(2)	Co(1)−Co(3)−Co(2)	60.10(3)
Co(1)−B(1)−B(2)	65.2(4)	Co(1)−Co(3)−B(2)	51.0(2)
Co(1)−B(1)−B(3)	102.7(4)	Co(1)−Co(3)−B(3)	78.0(2)
Co(1)−B(1)−H(1)	124(4)	Co(2)−Co(3)−B(2)	78.0(2)

Kinetics In each case, a NMR tube capped with a septum was prepared by transferring 2 mL of a toluene solution of **1** of known concentration (by weight). After an initial ^{11}B spectrum was recorded at room temperature, each tube was heated at constant temperature for a measured period of time. ^{11}B NMR measurements were continued until **1** (reactant) was no longer detectable. Experiments were carried out at 323, 338, 348, and 363 K. The temperature range was limited since too high a temperature caused the decomposition of product **3** and too long a period of measurement gave poor mass balances attributed to decomposition of **3**.

Results and Discussion

Stable Products. The new cobaltaboranes isolated and characterized in this work are presented in Scheme 1. Considering the extensive known structural chemistry of cobaltaboranes, only the important aspects of the characterization and significant features of each new cluster are highlighted.

***nido*-1-(η^5-C_5Me_5)Co-2-(η^4-C_5Me_5H)CoB_3H_8 (1).** Two kinds of boron environments are observed in the ^{11}B NMR spectrum of compound **1**. In the coupled spectrum, the signal of intensity one clearly shows coupling to one terminal hydrogen whereas the other signal is a complex multiplet. The ^1H NMR spectrum (Figure 1) shows the presence of one η^4-C_5Me_5H cyclopentadiene ligand and one η^5-C_5Me_5 ligand. Three types of signals assigned to bridging hydrogens corresponding to a total of 5H are observed. The two broad signals of area 2 are easily assigned to BHB (δ −6.0) and BHCo (δ −15.7) framework hydrogens. Curiously, the resonance assigned to a CoHCo bridge hydrogen is only clearly observed at lower temperatures as a shoulder in the case of C_6D_6 as solvent but as a separated signal in CD_2Cl_2. Both the unexpected low field chemical shift of the CoHCo resonance and its sensitivity to temperature are not understood. In agreement with these data, the ^{13}C NMR data show eight kinds of carbons. Each signal was assigned by measuring the coupled spectrum and by comparison to the spectrum of $Fe(CO)_3$(η^4-1,3-butadiene).[27]

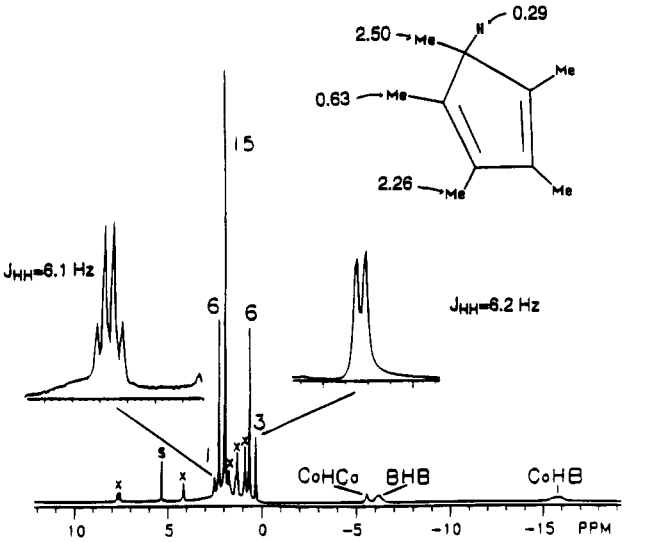

Figure 1. The ^1H NMR spectrum of *nido*-1-(η^5-C_5Me_5)Co-2-(η^4-C_5Me_5H)CoB_3H_8 (**1**) in CD_2Cl_2 at −15 °C. The chemical shift assignment for the (η^4-C_5Me_5H) ligand is shown.

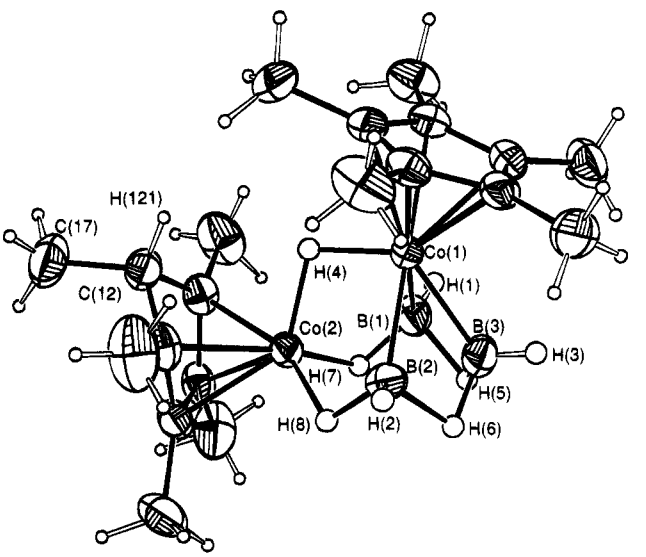

Figure 2. ORTEP drawing of *nido*-1-(η^5-C_5Me_5)Co-2-(η^4-C_5Me_5H)CoB_3H_8 (**1**).

The molecular structure of **1** is shown in Figure 2. All bond distances and angles are within the expected values (Table 2). The Co_2B_3 cluster core clearly constitutes a *nido* square pyramidal structure with geometric parameters similar to those of *nido*-1,2-$Fe_2(CO)_6B_3H_7$.[28] The isotropically refined hydrogen positions agree well with those required by the NMR data. The hydrogen attached to the η^4-cyclopentadiene ligand is positioned

(27) Gibson, D. H.; Ong, T.-S. *J. Organomet. Chem.* **1978**, *155*, 221.
(28) Andersen, E. L.; Haller, K. J.; Fehlner, T. P. *J. Am. Chem. Soc.* **1979**, *101*, 4390.

Scheme 1

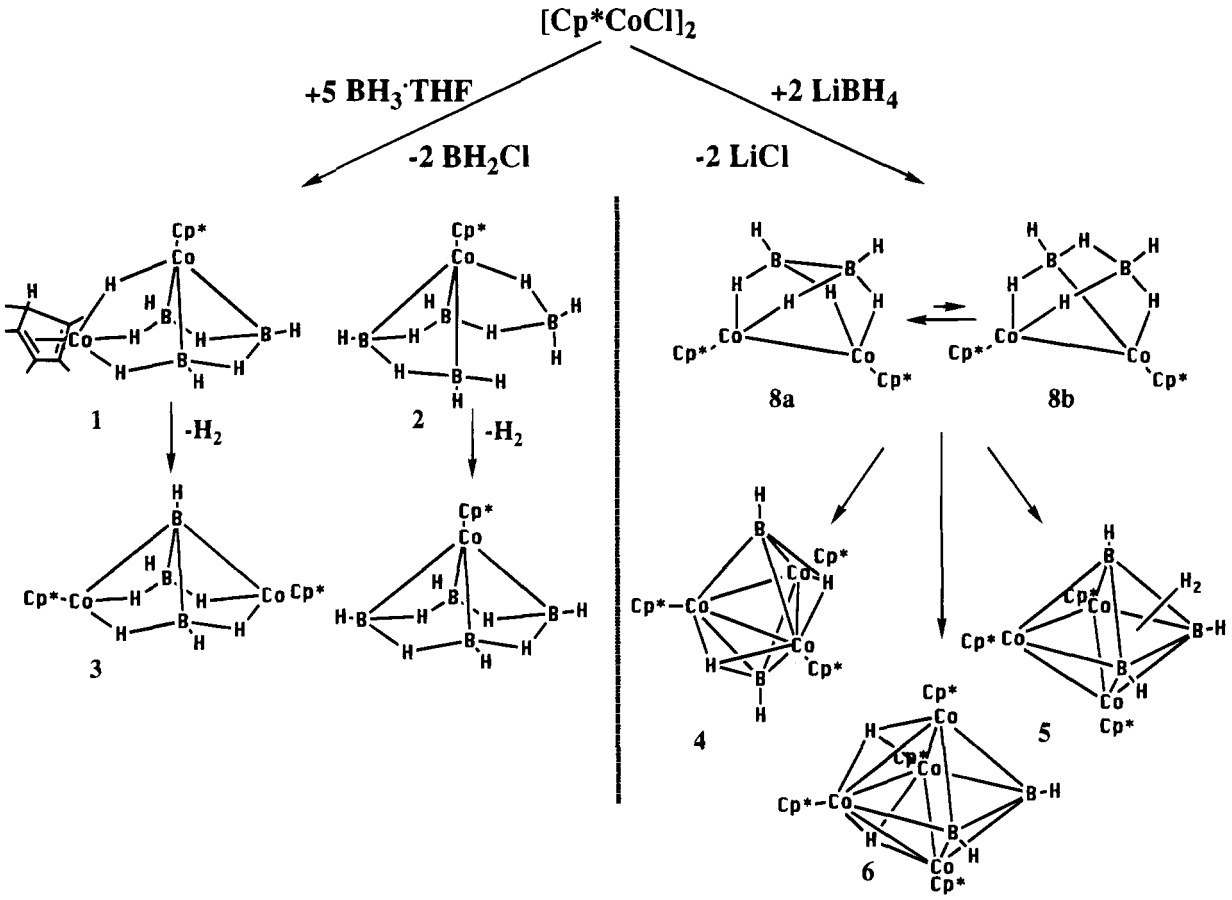

endo to the cluster and lies 2.9 Å from the closest carbon atom of η^5-C_5Me_5 ligand. This is slightly less than the sum of the van der Waals radii. Note that an extremely short interligand C−C distance of 2.3 Å would be present if a η^5-C_5Me_5 ligand is placed on the cobalt atom in the 2-position if all other atom positions are fixed. Presumably intramolecular ligand reduction and consequent bending of the methyl group away from the cage permits the metals to be adjacent. At the same time, the reduced framework electron count requires a *nido*-Co_2B_3 core geometry. This interplay of steric and electronic effects combined with a sufficient barrier for framework rearrangement (see below) lies behind the generation of this unusual structure.

The fact that the unique hydrogen atom on the η^4-C_5Me_5H ligand is adjacent (endo) to the cluster is important. Reduction of a Cp* ring in a bimolecular process would be expected to lead to η^4-C_5Me_5H ligand with an exo-hydrogen atom. Therefore, H atom transfer resulting in the production of **1** is intramolecular, i.e., it originates from a borane fragment coordinated to the cobalt dimer.

***arachno*-(η^5-C_5Me_5)CoB_4H_{10} (2).** Of the cobaltaboranes prepared, **2** is the most volatile and the most soluble in organic solvents. It is stable in the solid state but in solution slowly decomposes. The ^{11}B NMR spectrum exhibits two signals of equal intensity. The signal at +5.1 ppm is a doublet (one terminal hydrogen) whereas the signal at −5.7 ppm is a triplet (two terminal hydrogens). The ^1H NMR exhibits BHB and BHCo resonances. At low temperature, the BHB resonance consists of two partially overlapping resonances in a 2:1 intensity ratio (δ −3.6, 2H; -4.0 1H). The ^1H and ^{13}C NMR spectra show the presence of a single type of η^5-C_5Me_5 ligand.

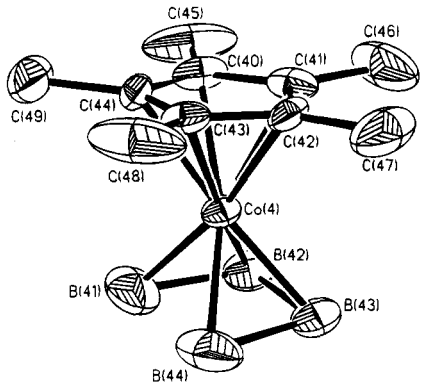

Figure 3. ORTEP drawing of *arachno*-(η^5-C_5Me_5)CoB_4H_{10} (**2**).

The structure of the framework of **2**, shown in Figure 3, reveals an *arachno*-core similar to that in pentaborane(11) with a Cp*Co fragment replacing the apical BH fragment (Table 4). Based on the NMR data, the framework hydrogen atoms are placed as shown in Scheme 1. Thus, they mimic the arrangement of hydrogens on the pentaborane(11) skeleton. A closely related metallaborane, [Ir(η^4-B_4H_9)(CO){$P(CH_3)_2C_6H_5$}$_2$], has been reported previously and has a MB_4 skeleton similar to that of **2**.[29] Pyrolysis of **2** at 70 °C results in H_2 loss and the clean formation of *nido*-1-(η^5-C_5Me_5Co)-B_4H_8 which was identified on the basis of its known spectroscopic parameters.[30]

(29) Boocock, S. K.; Toft, M. A.; Inkrott, K. E.; Hsu, L.-Y.; Huffman, J. C.; Folting, K.; Shore, S. G. *Inorg. Chem.* **1984**, *23*, 3084.

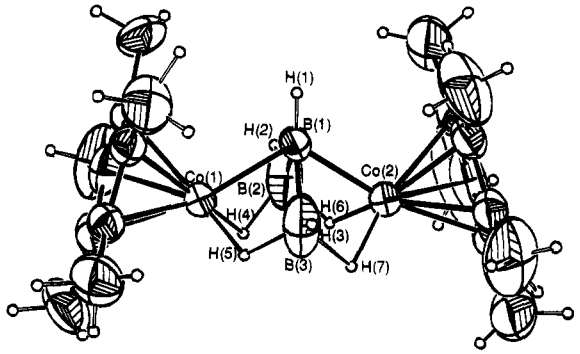

Figure 4. ORTEP drawing of *nido*-2,4-{(η^5-C_5Me_5)Co}$_2B_3H_7$ (**3**).

***nido*-2,4-{(η^5-C_5Me_5)Co}$_2B_3H_7$ (3).** The ^{11}B NMR spectrum of **3** exhibits two boron signals in the expected 2:1 ratio. In contrast to **1** the signals are now separated by 82 ppm with the signal of lower intensity at lower field. Also in contrast to **1** the ^1H and ^{13}C NMR spectra are simple indicating two equivalent Cp*Co fragments and four equivalent BHCo hydrogens. The integration of the signal at +6.28 ppm compared to the integration of methyl protons in η^5-C_5Me_5 ligand suggests assignment as one terminal hydrogen; however, no signal attributable to the other two terminal hydrogens was observed. The ^{13}C NMR spectrum shows two signals confirming the presence of only one kind of η^5-C_5Me_5 ligand.

The molecular structure of **3** is shown in Figure 4. All bond distances and angles are within expected ranges (Table 6). Interestingly, a *nido*-geometry is observed but the positions of the cobalt atoms have changed from 1,2- in **1** to 2,4- in **3**. At the same time the η^4-C_5Me_5H cyclopentadiene ligand in **1** becomes a η^5-C_5Me_5 ligand. Compound **3** is the first example of a *nido*-M_2B_3 core having the 2,4-isomeric framework. It is important to note that in terms of geometry *nido*-**1** effectively becomes *nido*-**3** by loss of the CoHCo and cyclopentadiene hydrogens (These specific hydrogens may not be the ones lost.). Also it is interesting that, whereas the apical ^{11}B resonance of B_5H_9 appears at high field, that of **3** is ≈110 ppm downfield of it. A high field position is characteristic of the apical position in the pentaborane(9) framework but it is the direct Co−B bonding in **3** that dominates the shift.[31]

The fact that the 2,4-isomer is observed rather than the 1,2-isomer is a clear indication that a repulsive interaction between the Cp* ligands on the hypothetical 1,2-{(η^5-C_5Me_5)Co}$_2B_3H_7$ decreases its stabilities relative to the 2,4-isomer. That is, 1,2-{Fe(CO)$_3$}$_2B_3H_7$ shows no tendency to rearrange up to its decomposition temperature[13] and, in the absence of steric effects, the 1,2-isomer should be the most stable of the three possibilities for the isolobal Cp*Co analog. As already noted, the conversion of a η^5-C_5Me_5 ligand to a η^4-C_5Me_5H ligand in the 2-position in **1** is required to avoid a repulsive interaction between two η^5-Cp* ligands. During the formation of **1** the barrier to this intramolecular ligand reduction is apparently much lower than that for cluster rearrangement to an *arachno*-2,4- or 2,5-dicobaltapentaborane(11). Hence, it is the first product observed.

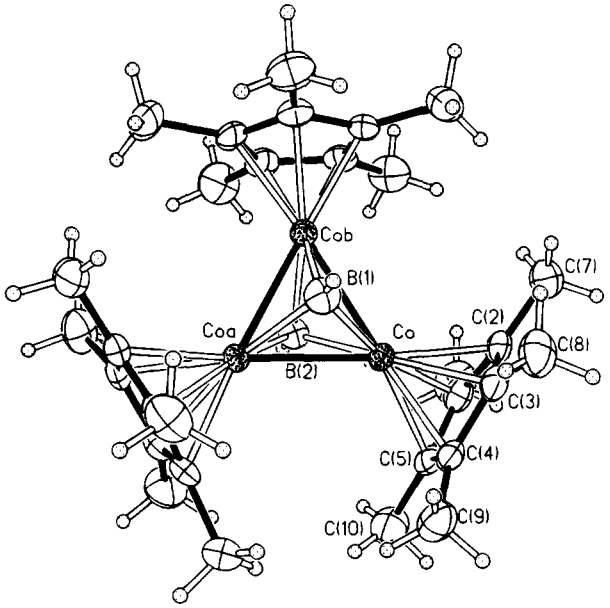

Figure 5. ORTEP drawing of *closo*-2,3,4-{(η^5-C_5Me_5)-Co}$_3B_2H_4$ (**4**).

***closo*-2,3,4-{(η^5-C_5Me_5)Co}$_3B_2H_4$ (4).** The ^{11}B NMR spectrum of **4** contains only one doublet at low field suggesting two equivalent BH fragments in a metal environment. The ^1H NMR spectrum shows a single Cp* methyl resonance, a single terminal BH resonance, and a resonance at high field (-20.76 ppm) due to two framework hydrogens. The $^{13}C\{^1H\}$ NMR spectrum also shows one type of Cp* ligand.

The molecular structure of **4** in Figure 5 shows a trigonal-bipyramidal cluster core with boron atoms in axial positions and cobalt atoms in equatorial positions. Bond distances and angles are within normal ranges (Table 8). Understandably, the framework hydrogens were not located because the crystallographic site symmetry requires a three-fold disorder in the two hydrogen positions.

The placement of the two framework hydrogens on the trigonal bipyramid is not obvious. In the ^1H NMR, they are equivalent and are fluxional down to the limit of observation in toluene-d_8, −90 °C; that is, there is only one Cp* signal observed. Moreover, the chemical shift δ −21 ppm is ambiguous as it could be assigned to either CoHCo or BHCo hydrogens. Selectively decoupled ^{11}B NMR spectra indicate that the framework hydrogen atoms are associated with boron; thus, CoCo edge-bridging hydrogens are ruled out. That leaves two possibilities which are CoB edge-bridging and Co_2B face-bridging hydrogens. Due to the relatively small coupling to boron and the relatively high chemical shift, the Co_2B face-bridging mode is preferred (Scheme 1).

***closo*-1,2,3-{(η^5-C_5Me_5)Co}$_3B_3H_5$ (5).** The molecular structure of **5** is shown in Figure 6. As **5** is the Cp* analog of *closo*-1,2,3-{(η^5-C_5H_5)Co}$_3B_3H_5$[32] and has a similar core structure (Table 10), little discussion of the structure is necessary. However, it is important to note that this *closo* structure does afford adjacent Cp* rings. As the square pyramidal *nido* structure is derived from an octahedral closo structure by the removal of a single vertex, the steric effect thought to be important for **1** might well be questioned. There is one important

(30) Venable, T. L.; Grimes, R. N. *Inorg. Chem.* **1982**, *21*, 887.
(31) Rath, N. P.; Fehlner, T. P. *J. Am. Chem. Soc.* **1988**, *110*, 5345.
(32) Pipal, J. R.; Grimes, R. N. *Inorg. Chem.* **1977**, *16*, 3255.

Scheme 2

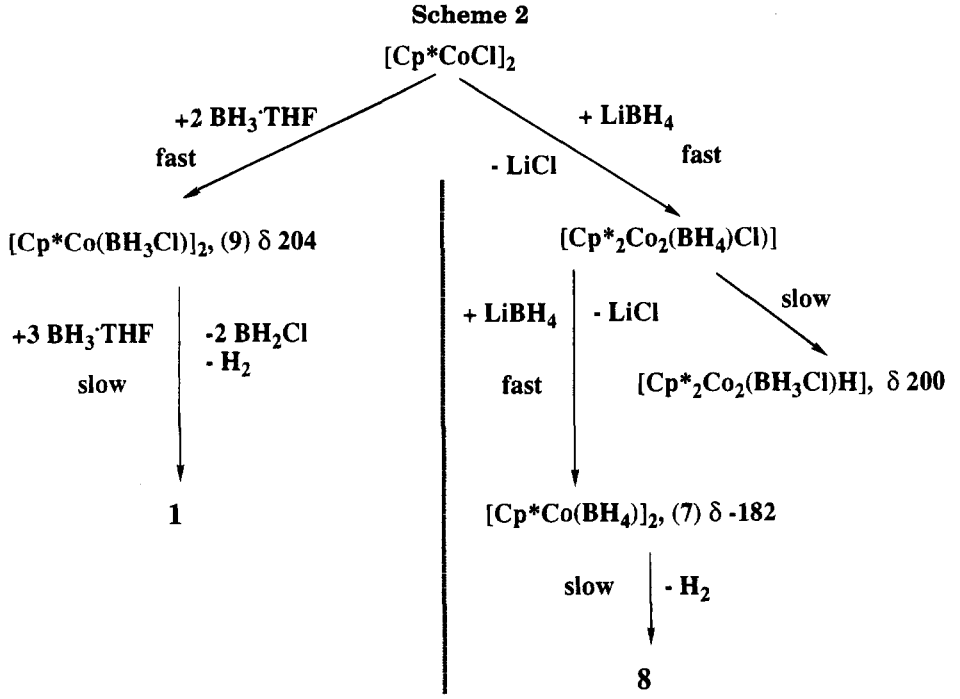

difference between the core structures of **1** and **5**. As exemplified by the structure of pentaborane(9), the presence of the bridging hydrogens on the open face causes the basal BH(term.) hydrogens to lie above the basal plane and closer to the apical boron atom than expected on the basis of a B_5H_5 fragment of a B_6H_6 octahedron. If one assumes that the BH(term.) vector corresponds to the vector from the Co atom to the centroid of the Cp* ring in the isolobal cobaltaboranes, then the steric requirement for adjacent Cp*Co fragments will be more severe for a square pyramidal structure with edge-bridging hydrogens than for an octahedral structure.

Metastable Products. The reaction of $[Cp^*CoCl]_2$ with $LiBH_4$ results in the immediate formation of a paramagnetic intermediate $[\{(\eta^5\text{-}C_5Me_5)Co\}(BH_4)]_n$ (**7**) where n is probably 2. With a reactant B, Co ratio > 1, excess BH_4^- and **7** are observed in the ^{11}B NMR (the formation of the diamagnetic products is relatively slow). With a B:Co ratio < 1, no BH_4^- is observed and another, even less stable, paramagnetic intermediate (δ 200) is observed in addition to **7** (δ −182). We suspect the latter to be $\{(\eta^5\text{-}C_5Me_5)Co\}_2(BH_3Cl)H$ with the Cl bound to boron although this is hardly certain (see below). These observations suggest the initial reaction is simply replacement of Cl^- with BH_4^-, for which there is ample precedent (Scheme 2).[33]

The paramagnetic intermediate **7** decays at room temperature into the diamagnetic $\{(\eta^5\text{-}C_5Me_5)Co\}_2B_2H_6$ (**8**). As shown in Figure 7, ultimately **4** forms as the major final product. The spectroscopic characterization of **8** is more complete than that for **7** and leads to a definitive structure. The ^{11}B NMR spectrum contains two resonances in a 1:1 ratio, suggesting two distinct boron environments whereas the ^1H NMR spectrum shows two kinds of BHCo bridges, one type of Cp* ligand (albeit a broad signal) and one kind of terminal BH. The IR spectrum confirms the presence of terminal BH. Variable temperature studies (Figure 8) showed that,

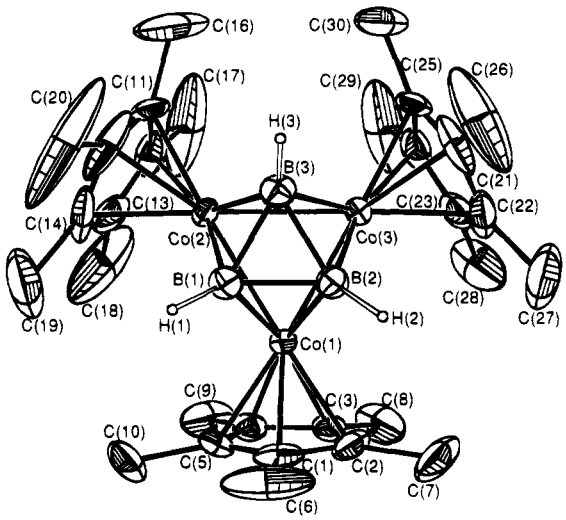

Figure 6. ORTEP drawing of *closo*-1,2,3-$\{(\eta^5\text{-}C_5Me_5)Co\}_3B_3H_5$ (**5**).

relative to the reference, the intensity of the signal of one boron (δ −7.5) increased and the other (δ 51) decreased as the temperature was raised. The overall change in the ratio of intensities δ 51/δ −7 went from 2.0 at −60 °C to 1.0 at 17 °C and the sum of the intensities remained constant. At low temperature, the proton signal at δ −10.6 ppm disappears, while the signal at −16.0 ppm remains intense and becomes sharp (Figure 8). The temperature variation of the ^1H signals is much more abrupt than with the ^{11}B signals suggesting that the tautomer associated with the δ −10.6 signal is fluxional. The observed change in relative intensities (but not positions) of signals with temperature suggests an equilibrium between tautomeric forms of **8**. Thus, the postulated structures (Scheme 1) are related to those of $Fe_2(CO)_6B_2H_6$[34] (isolobal with **8**) and $[(Cp^*Ta)_2(B_2H_6)(Br)_2]$. The latter compound also exhibits two tautomers in solution having hydrogen distributions like those

(33) Marks, T. J.; Kolb, J. R. *Chem. Rev.* **1977**, *77*, 263.

(34) Jacobsen, G. B.; Andersen, E. L.; Housecroft, C. E.; Hong, F.-E.; Buhl, M. L.; Long, G. J.; Fehlner, T. P. *Inorg. Chem.* **1987**, *26*, 4040.

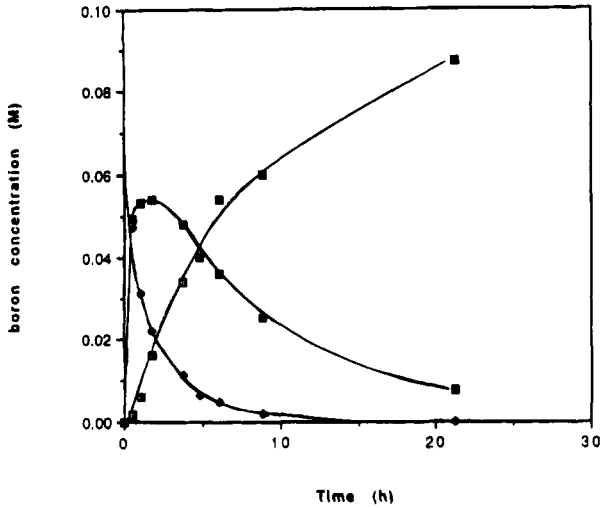

Figure 7. Plot of concentration vs time for $\{(\eta^5\text{-}C_5Me_5)\text{-}CoBH_4\}_2$ (**7**) (solid diamonds), $\{(\eta^5\text{-}C_5Me_5)Co\}_2B_2H_6$ (**8**) (solid squares), and *closo*-2,3,4-$\{(\eta^5\text{-}C_5Me_5)Co\}_3B_2H_4$ (**4**) (open squares) for the reaction of 1 equiv of $[Cp^*CoCl]_2$ with 1 equiv of $LiBH_4$.

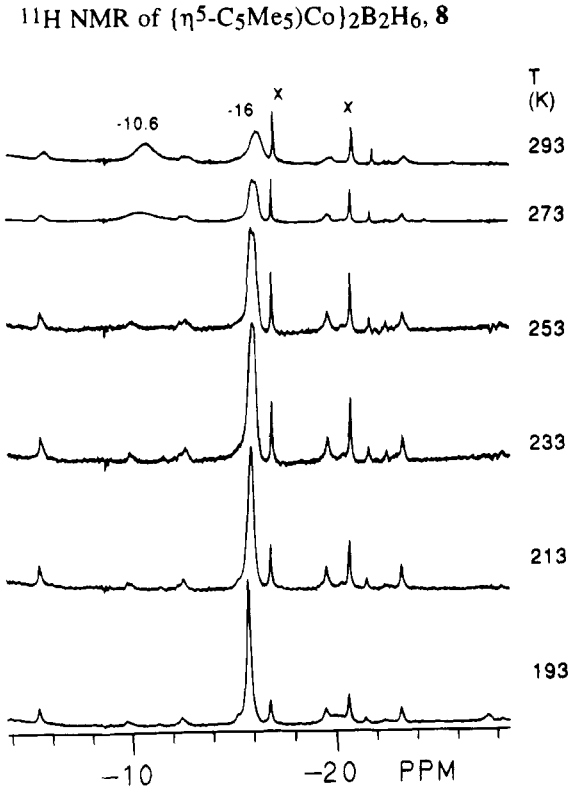

Figure 8. Variable temperature ^{1}H NMR spectra of $\{(\eta^5\text{-}C_5Me_5)Co\}_2B_2H_6$ (**8**) in the hydride region in $C_6D_5CD_3$. The peaks marked with x's are impurities.

proposed for **8**.[11] In the case of $[(Cp^*Co)_2B_2H_6]$, however, crystallization attempts have not been successful. The relative intensities of the ^{11}B NMR signals for the two tautomers as a function of temperature allow a difference in stability of 1 kcal/mol to be calculated, with structure **8a**, Scheme 1, being the more stable one.

The first diamagnetic molecule, **8**, in the $LiBH_4$ reaction is reactive under the preparative conditions and readily converts to cobaltaboranes with three or more Cp*Co fragments. These are more easily handled and are the first true isolated products. However, the data in Figure 7 exhibit the classic time behavior for a consecutive series of reactions showing that **8**, which contains the $Cp^*_2Co_2$ dimer fragment from the reactant, is intermediate in the formation of the more robust product **4**.

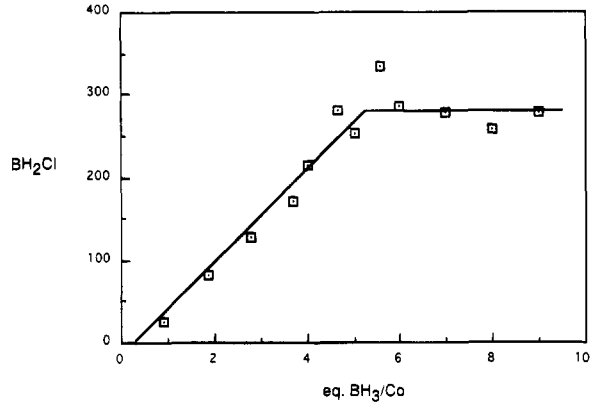

Figure 9. Plot of relative ^{11}B NMR integrations of BH_2Cl·THF formed vs equivalents of BH_3·THF used in reaction 1.

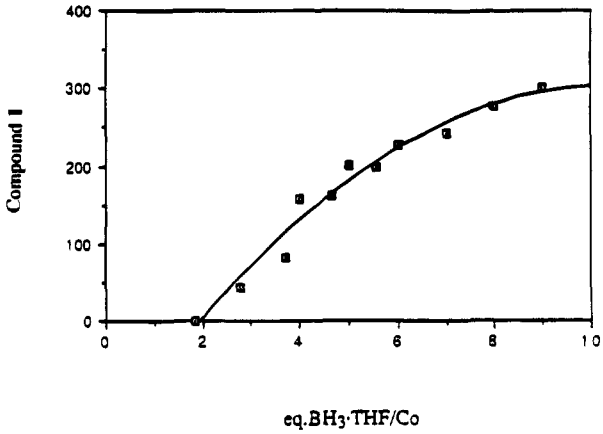

Figure 10. Plot of relative ^{11}B NMR integrations of *nido*-1-$(\eta^5\text{-}C_5Me_5)$Co-2-$(\eta^4\text{-}C_5Me_5H)CoB_3H_8$ (**1**) formed vs equivalents of BH_3·THF used in reaction 1.

The reaction of BH_3·THF with $[Cp^*CoCl]_2$ leading to **1** is accompanied by the formation of BH_2Cl. This was demonstrated unambiguously by following the reaction progress with ^{11}B NMR spectroscopy. Figure 9 demonstrates that ≈5 mol of BH_3 are required to maximize the formation of BH_2Cl. This is consistent with eq 1.

$$5BH_3\text{·THF} + [Cp^*CoCl]_2 \rightarrow 2BH_2Cl + \textit{nido}\text{-1-}(\eta^5\text{-}C_5Me_5)\text{Co-2-}(\eta^4\text{-}C_5Me_5)CoB_3H_8\ (\mathbf{1}) \quad (1)$$

In the process of observing this reaction, a paramagnetic intermediate (**9**) (^{11}B, δ 204; ^{1}H, δ 51) was observed to grow in before BH_2Cl is observed and then decays away as **1** is formed. A plot of **1** formed per mole of BH_3 (Figure 10) exhibits a threshold showing that 2 mol of BH_3 react rapidly with $[Cp^*CoCl]_2$ before any **1** is observed. Separate experiments show that the intermediate **9** decomposes in the absence of BH_3, reacts with BH_3 to form **1**, and reacts with $[Cp^*CoCl]_2$ on heating to form some **4**. These data, along with that on **7** suggest that **9** is $[\{(\eta^5\text{-}C_5Me_5)Co\}(BH_3Cl)]_2$. The downfield ^{11}B shift of **9** relative to **7** is consistent with the presence of Cl on boron, i.e., in diamagnetic BH_3Cl^- the ^{11}B resonance is calculated to be 11 ppm downfield of that of BH_4^-.[35] It is for this reason that we formulate the low field intermediate in the borohydride reaction

as $\{(\eta^5\text{-}C_5Me_5)Co\}_2(BH_3Cl)H$ rather than $\{(\eta^5\text{-}C_5Me_5)Co\}_2(BH_4)Cl$.

These observations are summarized in Scheme 2. Together they provide a chemically reasonable connection between the reactants and the first stable products. On the other hand, it is known that $[Cp^*CoCl]_2$ is partially dissociated in polar solvents and, thus, the reactivity of mononuclear fragments must also be considered.[36] The 1,2-disposition of the Co atoms of **1** and its instability with respect to **3** with a 2,4-disposition of metal fragments provides unambiguous evidence that it is the cobalt dimer rather than mononuclear species that reacts with borane. That is, if a monomeric solvated Cp*CoCl fragment were the precursor of **1**, an isomeric form with nonadjacent metal vertices, or even **3**, would be expected to be formed directly. The fact that **2**, which might originate from dissociation of $[Cp^*CoCl]_2$, is only observed in low yield is consistent with high dimer reactivity.

Conversion of 1 to 3. Heating **1**, which has a *nido* geometry, results in **3** which also possesses a *nido* geometry. In the process of losing H_2 a cluster framework rearrangement takes place such that the 1,2-dicobaltapentaborane is converted into a 2,4-dicobaltapentaborane. On the other hand, heating **2** (the *arachno*-monocobalt analog of **1**) leads to the quantitative (by NMR) formation of *nido*-1-$Cp^*CoB_4H_8$. Clearly there is a substantial difference between the two systems. If one had no geometric information, the natural tendency would be to interpret the molecular formula of **1** as arachno, i.e., $Cp^*_2Co_2B_3H_9$, with the possibility of H_2 loss leading to *nido*-$Cp^*_2Co_2B_3H_7$. As noted above, in the absence of large steric effects, the 1,2-isomer is expected to be more stable than the 2,4-isomer. The unusual features of this reaction coupled with the ease of synthesis of **1** caused us to carry out a kinetic study in order to probe in more detail the mechanistic aspects of this cluster dehydrogenation *cum* rearrangement.

Rates of reaction (eq 2) were measured by ^{11}B NMR and the integrals of both **1** and **3** (product) were evaluated as a function of time. There was no evidence for any intermediates in the ^{11}B NMR spectra at any

$$1\text{-}(\eta^5\text{-}C_5Me_5)Co\text{-}2\text{-}(\eta^4\text{-}C_5Me_5H)CoB_3H_8 \rightarrow 2,4\text{-}\{(\eta^5\text{-}C_5Me_5)Co\}_2B_3H_7 + H_2 \quad (2)$$

stage in the reaction. First order plots were linear over 4 half-lives and independent of initial concentration although the latter was only varied ≈40%. Typical data and a table of rate constants are given in the supplementary material. Rate constants derived from formation of product are systematically higher than those based on loss of reactant. As the latter require no relative sensitivity correction they are probably more accurate. However, all data give Arrhenius parameters of $A = 10^{13\pm1}$ s^{-1} and $E_A = 26.5 \pm 2$ kcal/mol (Figure 11). There was no significant difference in the rate constants measured under 1 atm of N_2 vs H_2 at a fixed temperature. Attempted photolytic activation of **1** resulted in decomposition. The activation parameters, particularly the frequency factor, suggest a fairly tight

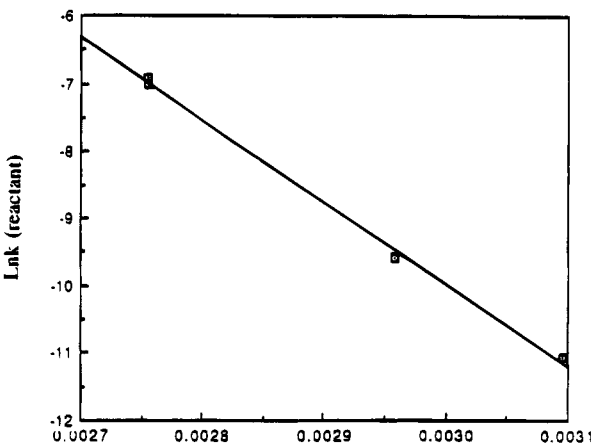

Figure 11. Arrhenius plot of the first order rate constant for reaction 2 derived from loss of reactant **1**.

activated complex for this apparent unimolecular diatomic elimination reaction and the observed value is consistent with those observed for related reactions.[37]

The 5-atom *nido*-framework is fairly resistant to rearrangement. For the B_5H_9 framework, mechanistic information obtained with appropriately labeled frameworks is available for rearrangement promoted by a Lewis base.[38,39] In the rearrangement of the B_5H_9 framework, the Lewis base coordinates and opens the cage at a basal edge thereby promoting BH fragment interchange via diamond-square-diamond (dsd) processes. Loss of the base and reclosing of the cage leads to rearranged B_5H_9.

This detailed mechanism for framework rearrangement provides the key to the formulation of a reasonable pathway for reaction 2. That is, **1** has an apparent *arachno* molecular formula but a real *nido* geometry and it therefore contains internally the equivalent of the pair of electrons provided by the Lewis base in the B_5H_9 rearrangement. That is, if the methylene hydrogen on the η^4-C_5Me_5H ligand, which is endo to the cage, is transferred to the framework with conversion to a η^5-C_5Me_5 ligand, the six skeletal bonding pairs of **1** increases by one and the cage should open. Thus, we suggest the mechanism shown in Scheme 3 in which a real *arachno* structure of **1** is accessed via a rapid equilibrium. Because of the steric interaction between the two Cp*Co fragments (see above) this intermediate is at high energy and either rapidly returns to **1** or undergoes a dsd rearrangement as shown. H_2 elimination from the second intermediate would lead to irreversible formation of **3**. It follows that formation of **1** from $[Cp^*CoCl]_2$ and borane also takes place via the first *arachno* intermediate in Scheme 3. If so, under the preparative conditions (low temperature) this intermediate would undergo intramolecular ligand reduction preferentially over H_2 loss and rearrangement. Synthesis at higher temperatures would lead directly to the formation of **3**.

In principle, the second intermediate should have minimal steric repulsion between the Cp*Co fragments and, as it is the analog of **2**, might be expected to have some stability. However, we observe no sign of such a

(35) Kidd, R. G. In *NMR of Newly Accessible Nuclei*; P. Laszlo, Ed.; Academic Press: New York, 1983; Vol. 2; p 49.
(36) Kölle, U.; Fuss, B.; Belting, M.; Raabe, E. *Organometallics* **1986**, *5*, 980.
(37) Benson, S. W. *Thermochemical Kinetics*; John Wiley: New York, 1968.
(38) Gaines, D. F. *Acc. Chem. Res.* **1973**, *6*, 416.
(39) Gaines, D. F.; Coons, D. E. *J. Am. Chem. Soc.* **1985**, *107*, 3266.

Scheme 3

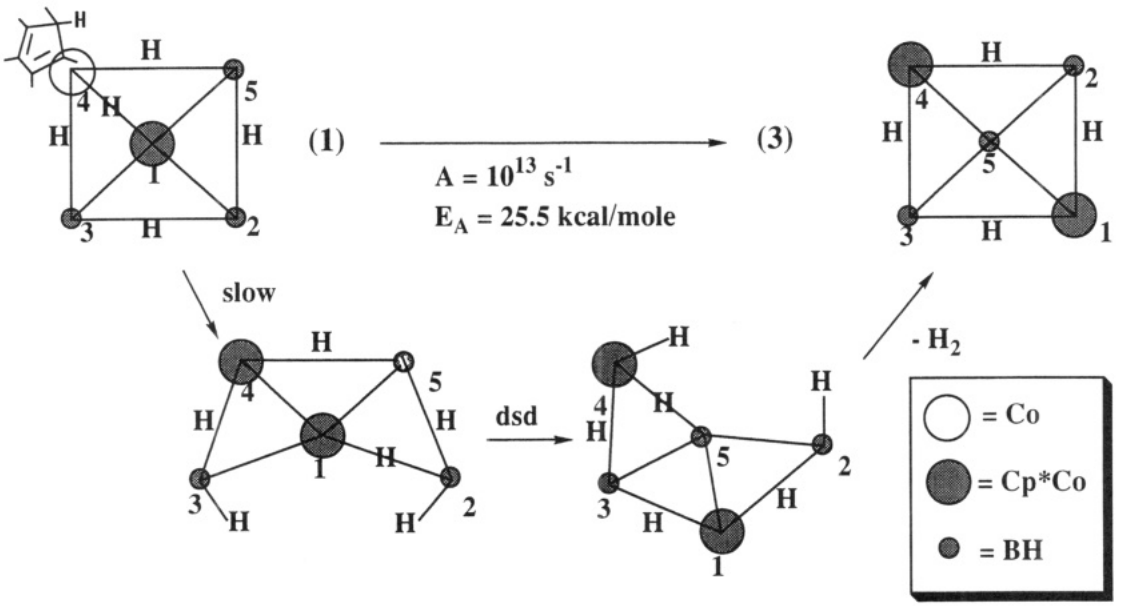

species during the reaction. Despite this, the crucial reaction barrier is associated with the H_2 elimination step. Otherwise, **3** would be observed instead of **1** in the preparative reaction. However, the transfer of the methylene hydrogen of the η^4-C_5Me_5H ligand to the Co_2B_3 skeleton is part of the activation process.

Conclusions

The results show that with an appropriate metal containing precursor, the number of metal atoms in the initial metallaborane can be controlled. This is true for either BH_3·THF or $LiBH_4$, albeit in the latter case the product is metastable. However, the number of boron atoms appears to be controlled by the reaction pathway which, in turn, depends on the boron source. Thus, a Co_2B_3 cage is accessed in good yield for BH_3·THF whereas a Co_2B_2 cage is found for $LiBH_4$. The utilization of this approach may permit many more types of metallaboranes to be synthesized.

The new cluster *nido*-1-(η^5-C_5Me_5)Co-2-(η^4-C_5Me_5H)-CoB_3H_8 (**1**) shows that the metal ligands can get involved in cluster chemistry in new ways. The apparent intramolecular hydrogenation of one Cp* ligand of the starting material leads to **1**. On raising the temperature, ligand dehydrogenation takes place concurrently with cluster cage rearrangement and cage dehydrogenation leading to *nido*-2,4-{(η^5-C_5Me_5)Co}$_2B_3H_7$ (**3**). None of this chemistry would have been observed if the synthesis had been carried out above 40 °C. The isolation of early products and the identification of metastable intermediate products has permitted the formulation of a reasonable mechanistic pathway.

Acknowledgment. The support of National Science Foundation is gratefully acknowledged.

Supplementary Material Available: Crystal data, experimental details, tables of crystal data, atomic positional and displacement parameters, selected distances and bond angles for **2** and **5**, a figure showing the four symmetry-independent molecules of **2**, and a graph of typical rate data and a table of rate constants for reaction 2 (27 pages). Ordering information is given on any current masthead page.

OM940482L